

TITLE: Allergic inflammation triggers dyslipidemia via IgG signalling

AUTHORS: Nieves Fernández-Gallego^{1,2#}, Raquel Castillo-González^{1,3#}, Lucía Moreno-Serna², Antonio J. García-Cívico^{4,5}, Elisa Sánchez-Martínez², Celia López-Sanz², Ana Luiza Fontes⁶, Lúgia L. Pimentel⁶, Ana Gradillas⁵, David Obeso^{4,5}, Marta Ramírez-Huesca¹, Ignacio Ruiz-Fernández¹, Emilio Nuñez-Borque⁷, Yolanda R. Carrasco⁸, Borja Ibáñez^{9,10,11}, Pilar Martín^{1,11}, Carlos Blanco¹², Coral Barbas⁵, Domingo Barber⁴, Luis M. Rodríguez-Alcalá⁶, Alma Villaseñor^{4,5}, Vanesa Esteban^{7,13}, Francisco Sánchez-Madrid^{1,2,11}, Rodrigo Jiménez-Saiz^{2,8,14,15*}

AFFILIATIONS:

¹Vascular Pathophysiology Area, Centro Nacional de Investigaciones Cardiovasculares (CNIC), 28029 Madrid, Spain

²Department of Immunology, Instituto de Investigación Sanitaria Hospital Universitario de La Princesa (IIS-Princesa), Universidad Autónoma de Madrid (UAM), 28006 Madrid, Spain

³Department of Immunology, Ophthalmology and Ear, Nose and Throat (ENT), Universidad Complutense, 28040 Madrid, Spain.

⁴Department of Basic Medical Sciences, Faculty of Medicine, Instituto de Medicina Molecular Aplicada (IMMA), Universidad San Pablo-CEU, CEU Universities, 28668 Madrid, Spain

⁵Centro de Metabolómica y Bioanálisis (CEMBIO), Faculty of Pharmacy, Universidad San Pablo-CEU, CEU Universities, 28668 Madrid, Spain

⁶Universidade Católica Portuguesa, CBQF - Centro de Biotecnologia e Química Fina – Laboratório Associado, Escola Superior de Biotecnologia, 4169-005 Porto, Portugal

⁷Department of Allergy and Immunology, Instituto de Investigación Sanitaria Fundación Jiménez Díaz (IIS-FJD), Universidad Autónoma de Madrid (UAM), 28040 Madrid, Spain

⁸Department of Immunology and Oncology, Centro Nacional de Biotecnología (CNB)-CSIC, 28049 Madrid, Spain

⁹Myocardial Pathophysiology Area, Centro Nacional de Investigaciones Cardiovasculares (CNIC), Madrid, Spain

¹⁰Department of Cardiology, Instituto de Investigación Sanitaria Fundación Jiménez Díaz (IIS-FJD), 28040 Madrid, Spain

¹¹CIBER de Enfermedades Cardiovasculares (CIBERCV), Instituto de Salud Carlos III, 28029 Madrid, Spain

¹²Department of Allergy, Instituto de Investigación Sanitaria Hospital Universitario de La Princesa (IIS-Princesa), 28006 Madrid, Spain

¹³Faculty of Medicine and Biomedicine, Universidad Alfonso X El Sabio, 28037 Madrid, Spain

¹⁴Department of Medicine, McMaster Immunology Research Centre (MIRC), Schroeder Allergy and Immunology Research Institute (SAIRI), McMaster University, Hamilton, ON, L8N 3Z5, Canada

¹⁵Faculty of Experimental Sciences, Universidad Francisco de Vitoria (UFV), 28223 Madrid, Spain

#First co-authors.

CONTACT INFORMATION:

*Correspondence to: Rodrigo Jiménez-Saiz, PhD. Department of Immunology, Instituto de Investigación Sanitaria Hospital Universitario de La Princesa (IIS-Princesa), Diego de León 62, Madrid 28006, Spain.

Email address: rodrigo.jimenez@ufv.es / carlosrodrigo.jimenez.externo@salud.madrid.org

SUMMARY

Allergic diseases begin early in life and are often chronic, thus creating an inflammatory environment that may lead to metabolic disorders, although the underlying mechanisms remain incompletely understood. Here, we show that allergic inflammation induces diet-independent dyslipidemia in a mouse model of allergy and atherosclerosis. Using untargeted lipidomics in mouse plasma, we found that allergic inflammation induces a unique lipid signature that extends beyond acute and late inflammation and that is characterized by triglyceride (TG) changes in circulation. Alterations in blood TGs following an allergic reaction are independent of T-cell-driven late phase inflammation. On the contrary, the humoral component is sufficient to induce a TG increase and a unique lipid profile through the IgG-mediated alternative pathway of anaphylaxis. Lastly, we demonstrated blood TG changes in patients after undergoing an allergic reaction. Overall, this study reveals the importance of IgG-mediated allergic inflammation insofar as it regulates lipid metabolism, which may contribute to atherosclerosis and, ultimately, to cardiovascular events.

INTRODUCTION

Type 2 immunity provides protection against parasites and non-microbial noxious substances and regulates several homeostatic processes^{1,2}. However, when it is directed toward innocuous antigens from food, pollen, animal dander, *etc.* it causes allergic diseases³. These begin early in life and are often chronic, thus creating an inflammatory ambient that may precede or exacerbate other pathologies⁴. In this regard, allergy has been associated with a higher risk of atherosclerosis^{5,6}, which

67 accounts for over 80% of deaths caused by cardiovascular disease, the major cause of mortality
68 worldwide⁷.

69 Atherosclerosis is a disease characterized by the chronic inflammation of blood vessels⁸. From an
70 immunological perspective, atherosclerosis is predominantly driven by type 1 immunity, which is
71 opposed to the hallmark type 2 identity of allergic disease⁹. Intriguingly, rather than counteracting
72 atherosclerosis, allergy seems to exacerbate this condition¹⁰. Atherosclerosis begins early in life,
73 typically associated with dyslipidemia, progresses slowly, and can remain silent until clinical
74 manifestations arise in the form of ischemic heart disease and/or stroke^{11,12}.

75 The pathology of allergic disease is heterogeneous and can generally be divided into two phases
76 that are initiated by allergen exposure in a time-dependent manner. Upon allergen exposure, acute
77 allergic reactions take place within minutes, or even seconds, via IgE (classical pathway)¹³ or,
78 although less characterized in humans, via IgG (alternative pathway)^{14,15}. Then, late phase
79 inflammation develops hours, or even days, after allergen encounter, and it is mainly orchestrated
80 by CD4 Th2 cells¹⁶.

81 Recent studies in human allergic patients point towards metabolic alterations linked to allergic
82 disease¹⁷⁻²⁰. Also, a recent transcriptomic study in the blood of healthy donors found an association
83 between triglyceride (TG) levels and canonical genes of type 2 immunity²¹, which underscores the
84 existence of an interplay between allergic disease and lipid metabolism. Yet the relationship of
85 allergic disease and its different phases to metabolic changes and, particularly, to dyslipidemia, the
86 main risk factor of atherosclerosis, remains poorly understood.

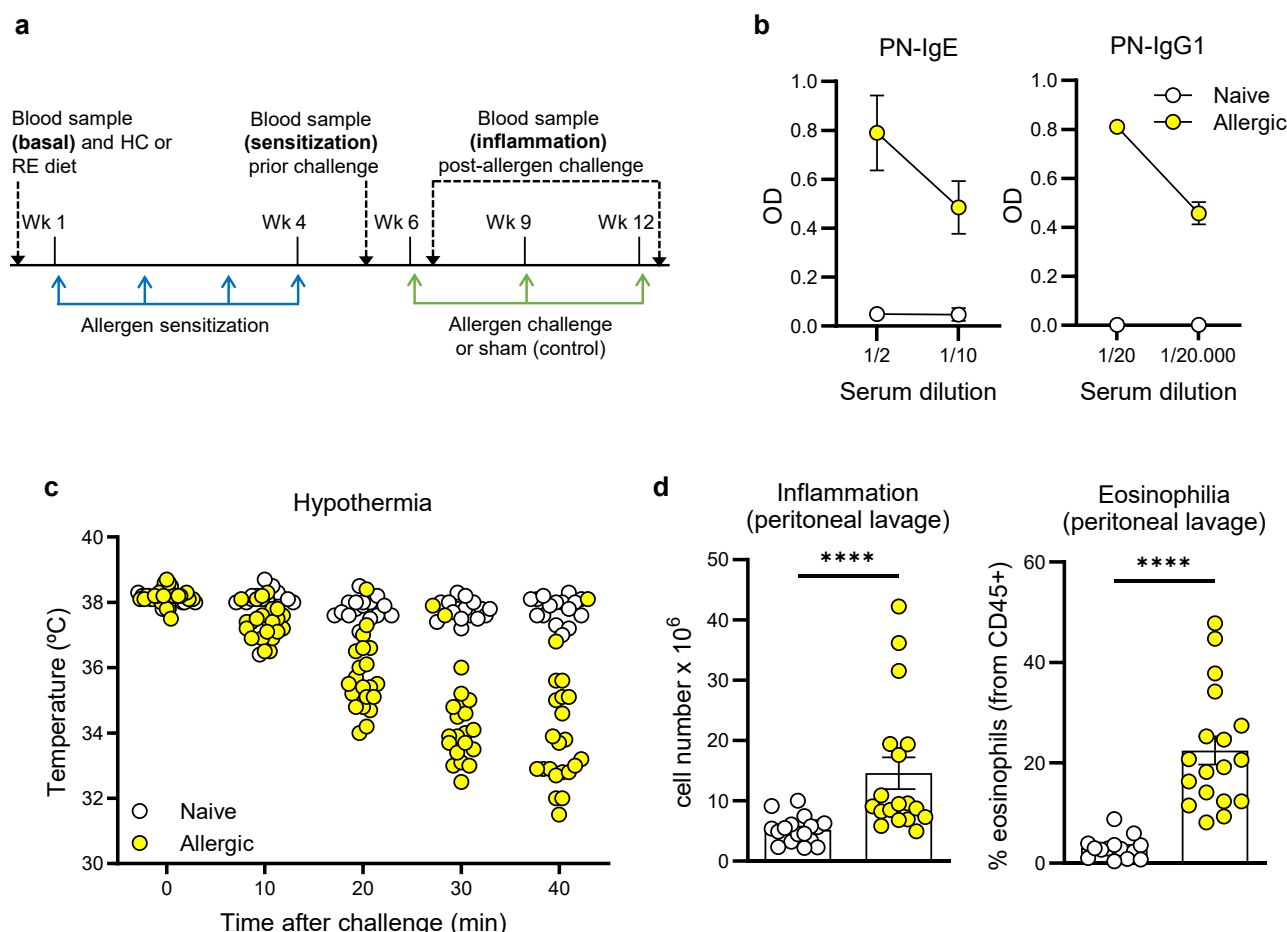
87 Here, we investigated the impact of allergic inflammation in dyslipidemia, and the effect of the diet,
88 in a murine model of allergy and atherosclerosis. Furthermore, we ascertained the contribution of
89 acute and late phase inflammation to allergic dyslipidemia using cell-depleting strategies and passive
90 sensitization models and delved into the role of the classical and alternative anaphylaxis pathways.
91 Moreover, untargeted lipidomics were applied to define the lipid fingerprint of allergic inflammation.
92 Lastly, we evaluated changes in serum TG levels in patients undergoing allergic reactions. Overall,
93 this study reveals the importance of humoral allergic inflammation in lipid metabolism, which may
94 contribute to atherosclerosis and, ultimately, to cardiovascular events.

95

96 RESULTS

97 **Allergic reactivity causes a diet-independent increase in blood triglycerides.** To investigate the
98 clinical association between allergic disease and atherosclerosis, we applied a well-established
99 model of allergy and anaphylaxis^{22,23} in LDL receptor-deficient mice (LDLr KO) (**Fig. 1a**). This mouse
100 strain is prone to atherosclerosis, particularly when fed a high cholesterol (HC) diet²⁴. Following

101 sensitization, LDLr KO mice developed high serum levels of allergen-specific IgE and IgG1 (**Fig. 1b**),
 102 and acute allergic responses upon allergen challenge, measured as changes in core temperature
 103 (**Fig. 1c**). Also, allergic mice exhibited late phase inflammation, characterized by eosinophilia in the
 104 peritoneal cavity (site of challenge) (**Fig. 1d; Fig. S1**). Given that the blood lipid profile can inform of
 105 cardiovascular risk, we collected fasting blood samples at different time points of allergic pathology
 106 including baseline, after sensitization, and post-allergen challenge (**Fig. 1a**).



107 **Fig. 1 Allergic sensitization and clinical responses in atherosclerosis-prone mice.** **a** Protocol
 108 for allergen sensitization, challenge, and sample collection in LDLr KO mice fed a high cholesterol
 109 (HC) or regular (RE) diet. **b** Serum levels of peanut (PN)-specific IgE and IgG1 after sensitization of
 110 HC diet-fed naive (n=14) and allergic (n=15) mice. **c** Acute allergic response following allergen
 111 challenge measured as hypothermia in HC diet-fed naive (n=16) and allergic mice (n=22). **d** Late
 112 phase inflammation in the peritoneal lavage at 3 days post-allergen challenge quantified in terms of
 113 total cell number and eosinophilia in HC diet-fed naive (n=15) or allergic (n=18) mice. Data for **b** and
 114 **d** are presented as mean \pm s.e.m. In **c** and **d**, each dot represents an individual mouse. Statistically
 115 significant differences in **d** were calculated with the Mann-Whitney test (****p \leq 0.0001). Pool of 3
 116 independent experiments.

We did not observe any significant differences in the lipid profile of allergic and naive mice except for TGs, which were increased in the allergic group, but only after allergen challenge (**Fig. 2a**).

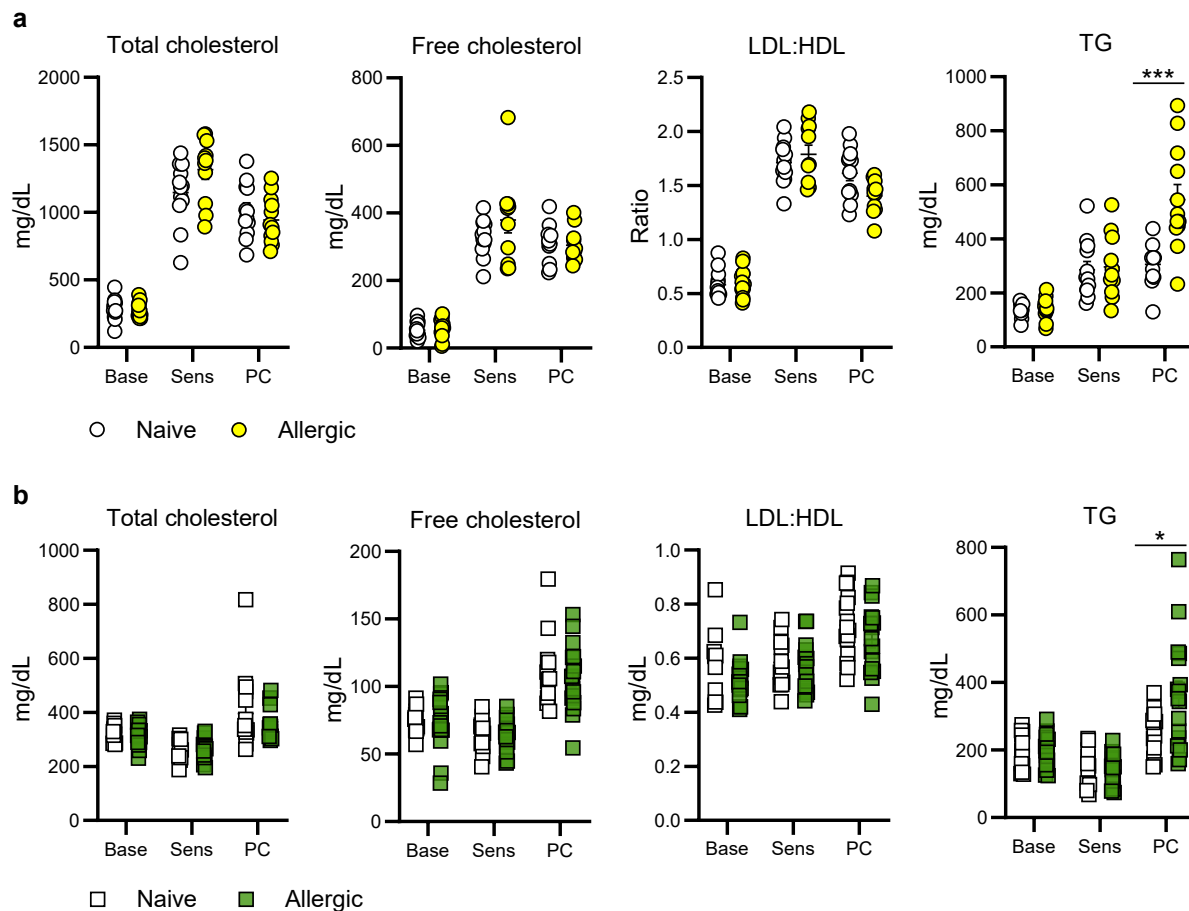


Fig. 2 Serum triglyceride (TG) levels increase following allergic inflammation. **a, b** Serum levels of total cholesterol, free cholesterol, LDL:HDL ratio and TGs determined at baseline (Base), after sensitization (Sens) and 3 days post-allergen challenge (PC) in naive and allergic mice fed a high-cholesterol (HC) diet (**a**) or a regular (RE) diet (**b**). The data shown in **a** include 12 naive and 12 allergic mice; the data shown in **b** include 15 naive and 17 allergic mice. Each dot represents an individual mouse. Data are presented as mean \pm s.e.m. Statistically significant differences between groups for each time point were calculated with the Mann Whitney test (* $p \leq 0.05$; *** $p \leq 0.0005$). Pool of 3 independent experiments.

The fact that elevated TG levels have been recently identified as a risk factor of subclinical atherosclerosis in the PESA study (an observational, longitudinal and prospective study with 4,000 patients), even in patients with normal LDL:HDL²⁵, prompted us to investigate these changes further. We questioned whether the systemic TG increase observed in allergic mice following allergen exposure was partly due to the HC diet used to study atherosclerosis or was inherent to allergic inflammation. To address this question, we followed a similar experimental design (**Fig. 1a**), but mice were fed a regular diet (RE) rather than a HC one. Also, we collected blood samples after the first

137 challenge, to assess lipid changes in the incipient stages of atherosclerosis. In agreement with the
138 previous data, we did not observe differences in the lipid profile of allergic and naive mice at different
139 phases of allergic pathology, except for TGs, which were again increased in the allergic group after
140 allergen challenge (**Fig. 2b**). Altogether, these results indicate that allergic inflammation induces a
141 systemic increase in blood TGs that is diet independent.

142

143 **Allergic inflammation causes a unique lipid signature in circulation.** The systemic increase in
144 serum TG levels following an allergic reaction was suggestive of more profound changes in the lipid
145 profile. Thus, we performed a comprehensive, kinetic blood analysis at different times post-allergen
146 (or PBS) exposure in allergic and naive mice under HC or RE diets, via untargeted lipidomics (**Fig.**
147 **3a**). The plasma samples, collected at 1-, 3-, and 7-days post-allergen or PBS challenge, were
148 treated for lipid extraction and were analysed using liquid chromatography coupled to mass
149 spectrometry (LC-MS). After curating the data with the respective quality assurance using the blanks,
150 the presence in samples and quality controls (QCs), and according to the coefficient of variance of
151 the QCs (<30%), we obtained 1,374 features including both positive and negative ionization modes.
152 Then, we assessed for the major separations between groups based on the overall lipid profile via
153 principal component analysis (PCA) models (**Fig. 3b**). As expected, the group on a RE diet
154 differentiated well from those on a HC diet at all time points. Interestingly, the lipid profile of naive
155 and PBS-challenged allergic mice on a HC diet was comparable and overlapping across the study,
156 which indicates that quiescent allergy, or atopy *per se*, does not alter the blood lipid profile.
157 Intriguingly, upon allergen challenge, the lipid profile of HC-diet-fed allergic mice became
158 increasingly different, as compared to that of naive mice or unchallenged allergic mice on a HC diet.
159 This effect became most obvious 7 days after inducing allergic inflammation, at which point the lipid
160 profile of allergen-exposed mice on a HC diet was clearly distinct from that of the rest of the groups
161 (**Fig. 3b**).

162

163

164

165

166

167

168

169

170

171

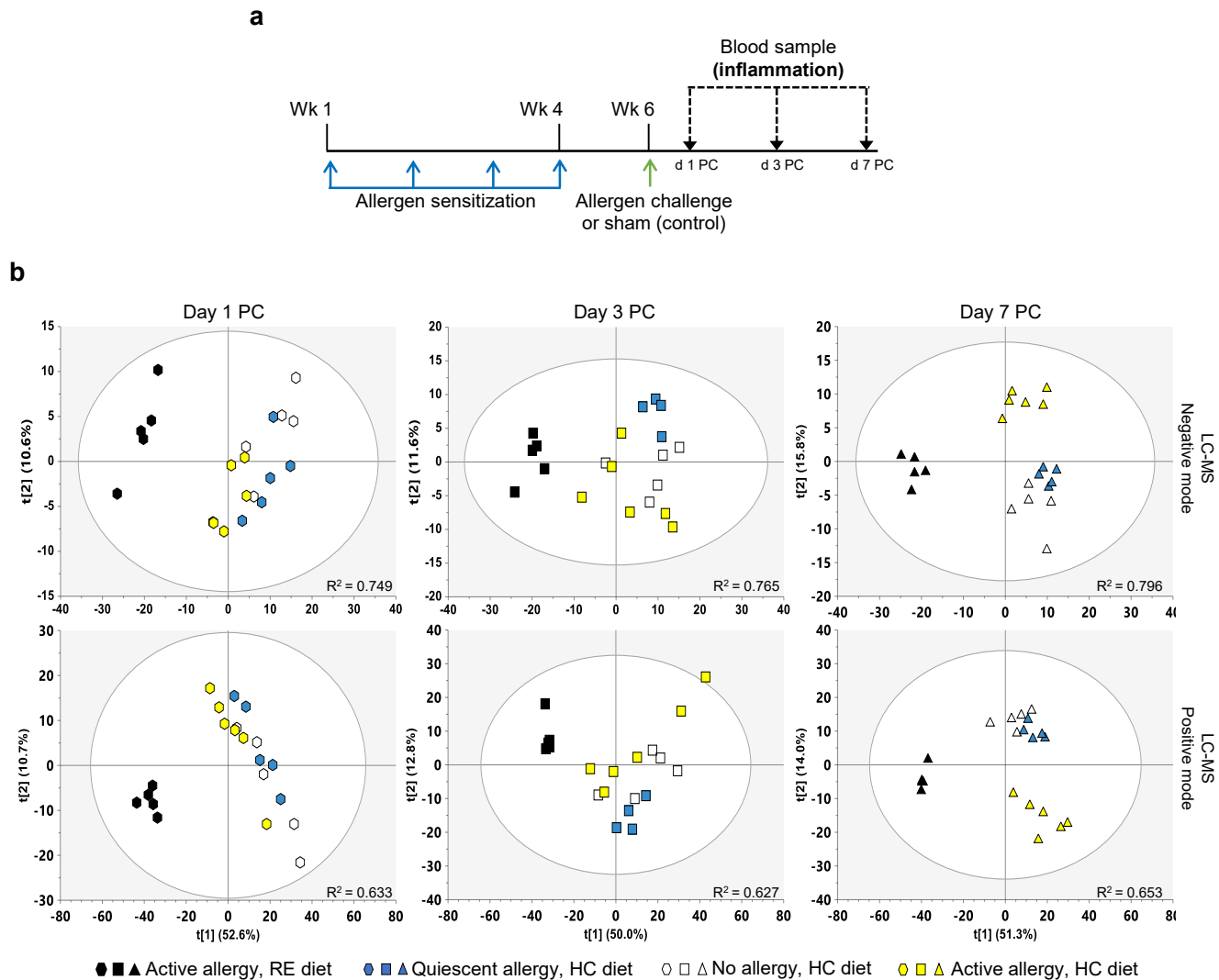
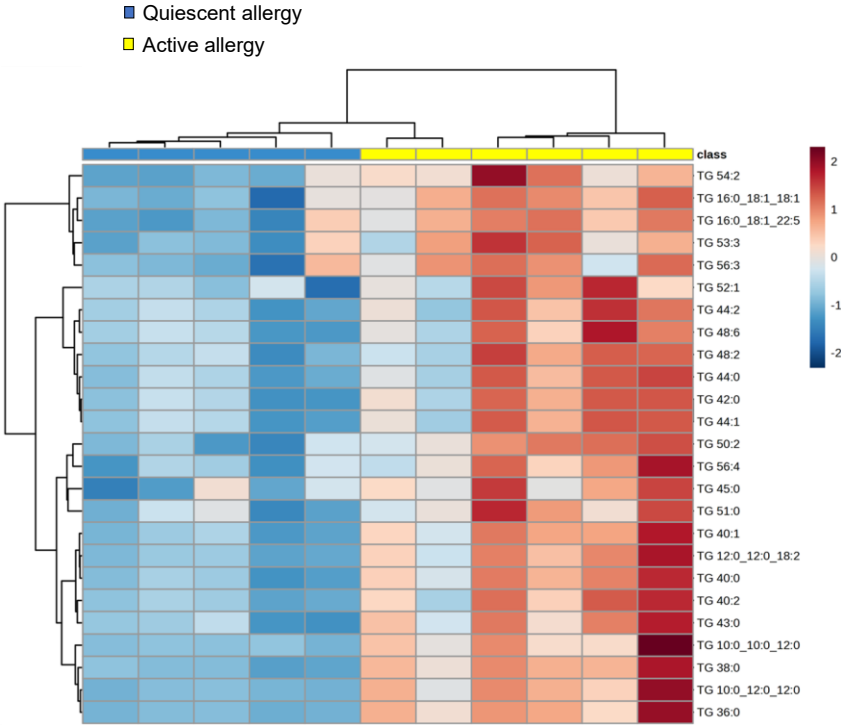
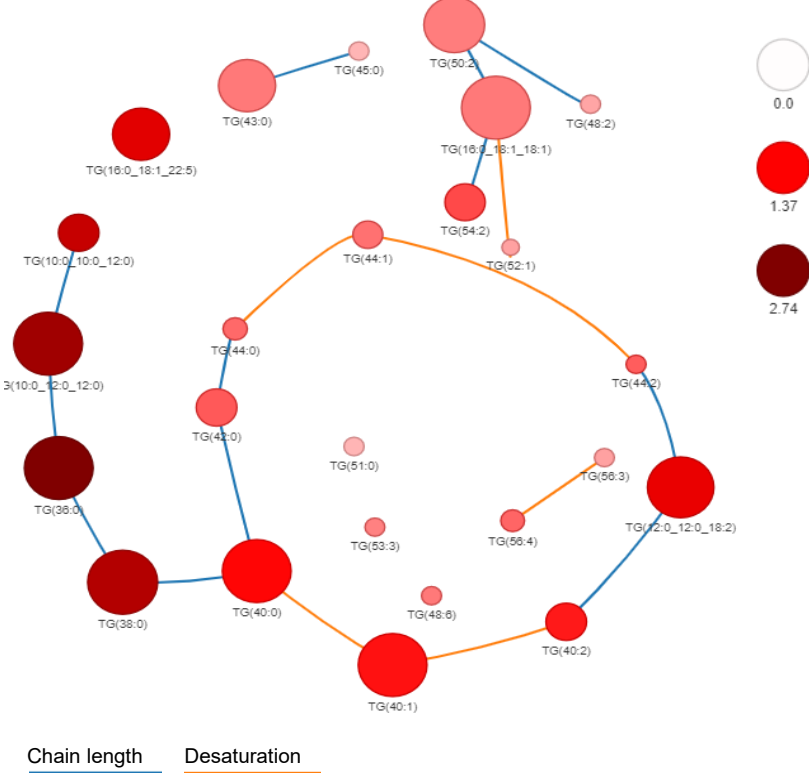


Fig. 3 Principal component analysis (PCA) models of the blood lipid profile at different phases of allergic pathology. **a** Protocol for allergen sensitization, challenge, and kinetic of blood sample collection in LDLr KO mice fed a high cholesterol (HC) or regular (RE) diet for lipidomics. **b** Unsupervised PCA model of liquid chromatography coupled to mass spectrometry (LC-MS) in negative and positive ionization mode of plasma samples from allergic or naive mice at different time points (1-, 3-, and 7-days post-allergen challenge, PC) of allergic pathology. The analysis includes allergen-challenged allergic mice on a RE diet (n=5, black color); non-challenged allergic mice on a HC diet (n=5, blue color); allergen-challenged naive mice on a HC diet (n=5, white color); and allergen-challenged allergic mice on a HC diet (n=6, yellow color). All data were unit variance (UV) scaled. The X and Y axis indicate the percentage of variability explained by each component. R^2 represents the total variability explained by the model to differentiate groups.

a



b



Chain length Desaturation

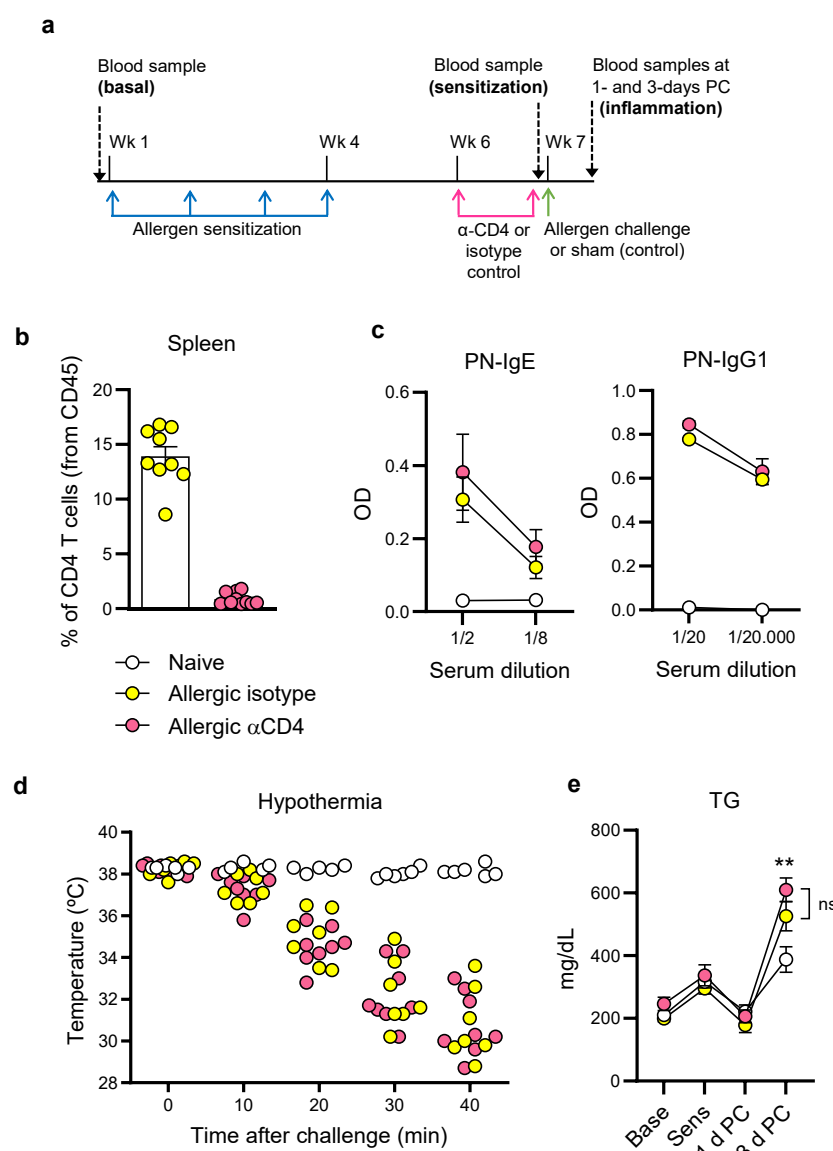
Fig. 4 Allergic inflammation induces a unique blood lipid profile of triglycerides (TGs). a Heatmap of the 25 specific TGs differentially expressed (p-value<0.05) between allergic mice with

193 quiescent allergy (non-challenged, blue color, n=5) and active allergy (allergen-challenged, yellow
194 color, n=6), fed a high cholesterol diet, at 7 days post-allergen challenge. The figure shows the
195 clustering results in the form of a dendrogram. Relative lipid abundance is represented along a color
196 gradient from blue (diminished in active allergy) to red (increased in active allergy). **b** Analysis of the
197 lipid metabolic networks of differentially expressed TGs in allergic mice with active allergy according
198 to their chain length, desaturation, and level of significance with LINEX. The intensity of the color
199 indicates the extent of TG upregulation; the sphere size indicates the level of significance of the
200 change according to the $-\log_{10}$ value FDR; the association between TGs according to their chain
201 length and level of desaturation are indicated by a blue and an orange line, respectively. TG 52:2
202 (TG 16:0_18:1_18:1); TG 56:6 (TG 16:0_18:1_22:5); FDR, false discovery rate.

203
204 In view of the unique lipid fingerprint exhibited by allergic mice 7 days after following allergen
205 exposure, we decided to compare it to the lipid profile of mice with quiescent allergy (sensitized but
206 not exposed to allergen), to better understand the impact of allergic inflammation on the lipid profile.
207 We detected 392 features that were significantly different in this comparison (adjusted p-value, p-
208 false discovery rate (FDR) < 0.05) including those from positive and negative ionization mode. Thus,
209 from these, we were able to identify 171 lipid species (**Fig. S2; Table S1**). Among them, we detected
210 25 specific TGs, all of which were increased during allergic inflammation (**Fig. 4a**). These TGs were
211 further analyzed using lipid metabolic networks according to their chain length, desaturation, and
212 level of significance (**Fig. 4b**). The analysis showed a cluster of TGs that have been associated with
213 cardiovascular disease (TG 54:2; TG 52:2; TG 50:2; TG 48:2)^{26,27}. In addition to these, but not
214 clustered together, TG 56:6, TG 56:4 and TG 53:3 have been also linked to cardiovascular disease²⁶
215 or risk factors of it (*i.e.*, hypertension, diabetes)²⁸. Collectively, these results show that allergic
216 inflammation yields a unique lipid signature, characterized by TG changes, that extends beyond the
217 acute phase of the pathology.

218
219 **Blood changes in triglyceride levels are independent of T-cell driven allergic inflammation.**
220 Allergic inflammation is characterized by an acute phase, which happens within minutes, or seconds,
221 following allergen exposure, and by a late phase, that occurs hours or even days after the reaction¹⁶.
222 The fact that the unique blood lipid signature triggered by allergic inflammation was detected days
223 after allergen exposure made us postulate that late phase inflammation was driving it. CD4 Th2 cells
224 orchestrate late phase inflammation, hence we decided to deplete CD4 T cells prior allergen
225 challenge to block it (**Fig. 5a**). We confirmed by flow cytometry that the antibody regime followed
226 was able to deplete CD4 T cells (**Fig. 5b; Fig. S3**), as previously reported^{22,29}. CD4 T-cell depletion
227 began 2 weeks after sensitization (1 week before allergen challenge) to avoid interfering with the
228 generation of allergen-specific IgE/IgG1, both of which contribute to the acute phase. Anti-CD4-
229 depleted and isotype-treated allergic mice showed comparable levels of allergen-specific IgE and

230 IgG1 (**Fig. 5c**). Likewise, both groups of allergic mice underwent anaphylaxis following allergen
 231 challenge (**Fig. 5d**), thus confirming that CD4 T-cell depletion had neither interfered with sensitization
 232 nor with acute allergic responses. The analysis of the blood lipid profile revealed that the TG peak
 233 previously observed during allergic inflammation remained intact despite CD4 T-cell depletion (**Fig.**
 234 **5e**). These data suggest that T-cell-driven late phase inflammation is not involved in the TG changes
 235 triggered by allergic inflammation.



236 **Fig. 5 Blood changes in triglyceride (TG) levels during allergic inflammation are independent**
 237 **of CD4 T cells.** **a** Protocol for allergen sensitization, CD4 T cell depletion, allergen challenge, and
 238 sample collection in LDLr KO mice fed a high cholesterol diet. **b** Flow cytometry analysis of CD4 T
 240 cell percentage in the spleen of anti-CD4-depleted and isotype-treated allergic mice. **c** Serum levels
 241 of peanut (PN)-specific IgE and IgG1 after sensitization. **d** Acute allergic responses following
 242 allergen challenge. **e** Serum TG levels determined at baseline (Base), after sensitization (Sens), and
 243 1- and 3- days post-allergen challenge (PC) in naive (n=8), and anti-CD4-depleted- (n=8) and

244 isotype-treated (n=7) allergic mice. Data for **b**, **c** and **e** are presented as mean \pm s.e.m. In **b** and **d**,
 245 each dot represents an individual mouse. Statistically significant differences in **e** were calculated
 246 with the Kruskal-Wallis test (**p \leq 0.005). Pool of 2 independent experiments.
 247

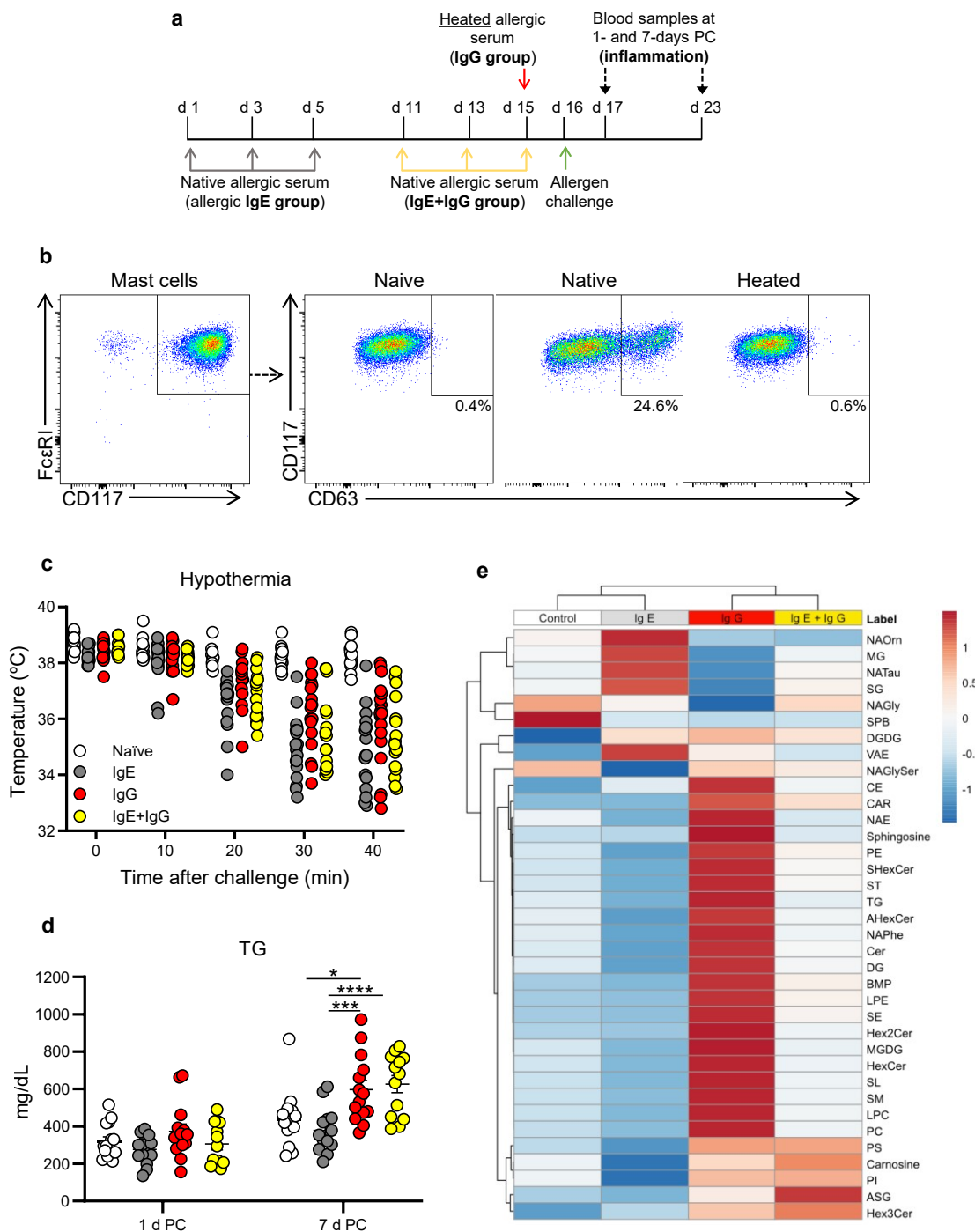
248 **Blood changes in TG levels during allergic inflammation are driven by IgG signalling.** The
 249 seemingly dispensable contribution of late phase allergic inflammation to dyslipidemia raised the
 250 possibility that this was triggered by the acute allergic response, which is strictly dependent on IgE
 251 and IgG1. To test this hypothesis, we devised a model of passive sensitization, which is based on
 252 the transfer of sera from allergic mice into naive recipients²². With this approach, only the humoral
 253 allergic machinery is transferred to naive mice, thus allowing for intact acute allergic responses and
 254 precluding Th2-driven late phase inflammation (**Fig. 6a**). Given that acute allergic responses can
 255 operate through the classical (IgE-mediated) and/or the alternative pathway (IgG-mediated), we
 256 examined the contribution of each pathway to blood TG levels.

257 Unlike other antibodies, IgE is irreversibly denatured at 57°C due to a heat-labile domain, which is
 258 not present in other antibody isotypes^{30,31}. We exploited this biochemical property to generate allergic
 259 sera without functional IgE. Following the heat-treatment of allergic sera, we observed a decrease
 260 in allergen-specific IgE levels as compared to the native allergic sera, while IgG1 levels remain
 261 unchanged (**Fig. S4a**). To ascertain if the remnants of denatured IgE were functional, we used a cell
 262 activation assay based on bone marrow-derived mast cells³². Mast cells sensitized with native
 263 allergic sera showed a dose-dependent activation following allergen stimulation by means of CD63
 264 expression detected by flow cytometry (**Fig. 6b; Fig S4b**). On the other hand, mast cells sensitized
 265 with heat-denatured allergic or naive sera did not increase CD63 expression after allergen
 266 stimulation, which was comparable to that of unstimulated cells (**Fig. 6b; Fig S4b**). These data
 267 demonstrate that the heat-treatment rendered allergen-specific IgE completely ineffective.

268 We also leveraged on the ability of anaphylactic IgE to remain bound, for months, to mast cells via
 269 its high affinity receptor (FcεRI), which contrasts with the rapid clearance of circulatory IgG from the
 270 circulation in a matter of days³³. Thus, resting the mice for 2 weeks after passive sensitization with
 271 allergic serum allows for blood IgG clearance and restricts anaphylaxis to the classical pathway²².
 272 Therefore, adjusting the sensitization time prior challenge as well as the type of sera used for it
 273 (native and heat-denatured), allowed us to induce anaphylaxis via the classical and/or alternative
 274 pathway (**Fig. 6a**). Upon challenge, all the allergic mice developed anaphylaxis to a similar level as
 275 determined by hypothermia (**Fig. 6c**), regardless of the sensitization sera used (native or heat-
 276 treated) and of the resting period prior challenge (1 day or 2 weeks). In line with the previous
 277 experiments, we did not observe changes between groups in the lipid profile following allergen
 278 challenge except for TGs (**Fig. 6d, Fig. S4c**). Interestingly, the group of allergic mice that underwent

279 anaphylaxis through the classical pathway (IgE-mediated) did not exhibit a TG peak. However, the
 280 groups of mice that experienced anaphylaxis through the alternative pathway (IgG) or a combination
 281 of both, showed a significant increase in blood TGs (**Fig. 6d**). Furthermore, we determined the lipid
 282 profile of plasma from these mice at 7-days post-allergen challenge via LC-MS analysis, as
 283 abovementioned. We identified 1,198 features that were grouped into 36 lipid classes for heatmap
 284 analysis (**Fig. 6e**). Remarkably, the naive and IgE groups were clustered together, while the IgE+IgG
 285 and IgG groups exhibited a profile that was more alike. The IgG group had a distinct lipid profile
 286 characterized by high peak intensities in TGs, as well as in compounds belonging to lipid classes
 287 such as sphingosine, N-acyl ethanolamines, lysophosphatidylethanolamines, hexosylceramides,
 288 monogalactosyldiacylglycerols, lysophosphatidylcholine, sulfonolipids, sphingomyelins,
 289 phosphatidylcholine, ceramides and diglycerides. In line with this, the univariate analysis showed
 290 that 456 lipids changed significantly (p -value<0.05) when comparing the IgG vs control group, while
 291 210 lipids did it in the IgE vs control group comparison (**Table S2**). Of note, 645 lipids were
 292 differentially expressed when comparing the IgG vs IgE group. These differences were attenuated
 293 when comparing the IgE+IgG group vs the IgE (239 lipids) or IgG (325 lipids) groups, due to their
 294 complementary profiles (**Table S2**). Altogether, these data indicate that allergic reactions are
 295 sufficient to induce a blood TG increase and a unique lipid signature that is mostly triggered by the
 296 IgG-mediated alternative pathway of anaphylaxis.

297



298

Fig. 6 Blood changes in triglyceride (TG) levels and in the lipid profile are driven by the IgG-mediated alternative pathway of anaphylaxis. **a** Protocol for passive sensitization with native and heated sera to induce anaphylaxis via de classical and/or the alternative pathway. **b** Activation assay with mast cells sensitized with naive sera, native allergic sera, and heat-treated allergic sera (representative dot plots of 4 independent experiments). **c** Acute allergic responses following allergen challenge of mice passively sensitized with naive sera (n=17) or allergic sera (native or

305 heated) to induce anaphylaxis via the classical (IgE; n=19) or alternative pathway (IgG; n=19), or
 306 both (IgE+IgG; n=18). **d** Serum TG levels measured at 1- and 7-days post-allergen challenge (PC)
 307 in passively sensitized mice. **e** Heatmap of the lipid species differentially expressed (p-value<0.05)
 308 at 7 days PC in different groups of passively sensitized mice (a pool of 5 individual samples from
 309 each group was analyzed in triplicate). The figure shows the clustering results in the form of a
 310 dendrogram. Relative lipid abundance is represented along a color gradient from blue (diminished)
 311 to red (increased). Data for **d** are presented as mean \pm s.e.m. In **c** and **d** and each dot represents
 312 an individual mouse from a pool of 3 independent experiments. Statistically significant differences in
 313 **d** were calculated with a two-way-ANOVA followed by Bonferroni's multiple comparisons test
 314 (*p \leq 0.05; ***p \leq 0.0005; ****p \leq 0.0001). AHexCer, acylhexosylceramides; ASG, acylsterylglucoside;
 315 BMP, bis(monoacylglycerol)phosphates; CAR, acyl carnitines; CE, cholesteryl esters; Cer,
 316 ceramides; DG, diacylglycerides; DGDG, digalactosyldiacylglycerol; Hex2Cer, dihexosylceramides;
 317 Hex3Cer, trihexosylceramides; HexCer, hexosylceramides; LPC, lysophosphatidylcholines; LPE,
 318 lysophosphatidylethanolamines; MG, monoacylglycerides; MGDG, monogalactosyldiacylglycerols;
 319 NAE, N-acyl ethanolamines; NAGly, N-acyl glycines; NAGlySer, N-acyl glyceryl serines; NAOri, N-
 320 acyl ornithines; NAPhe, N-acyl phenylalanines; NATau, N-acyl taurines; PC, phosphatidylcholines;
 321 PE, phosphatidylethanolamines; PI, phosphatidylinositols; PS, phosphatidylserines; SE, steryl
 322 esters; SG, sterylglucoside; SHexCer, sulfatides; SL, sulfonolipids; SM, sphingomyelins; SPB,
 323 sphingoid bases; ST, sterols; VAE, vitamin A fatty acid esters.

324

325

326 Allergic patients show increased blood triglyceride levels after an allergic reaction.

327 Considering the murine data, we decided to explore whether allergic reactions were able to induce
 328 blood TG changes in humans. Many common allergens are environmental and ubiquitous^{34,35}, which
 329 makes it difficult to control allergen exposure. In addition, subclinical exposures to the allergen might
 330 have an immunological impact too complex to be evaluated and controlled. Notwithstanding, we
 331 collected blood samples from 59 patients during the onset of an allergic reaction, and another one
 332 \geq 14 days later (**Fig. 7a**) to measure if allergic inflammation had induced changes in blood TG levels.
 333 Most of the patients presented hypersensitivity reactions of grade I and II severity³⁶, triggered by
 334 drugs or foods (**Table 1**). Given that some anti-inflammatory drugs may alter the blood TG levels³⁷,
 335 the initial sample was taken prior treatment of the reaction, and the second sample was taken at
 336 least 14 days later to allow for drug clearance. We also evaluated in different preclinical models of
 337 anaphylaxis that blood TG levels did not change shortly after the allergic reaction (data not shown)
 338 and remain unchanged for up to 24 h after it (**Fig. 4e**).

339

340

341

342

343

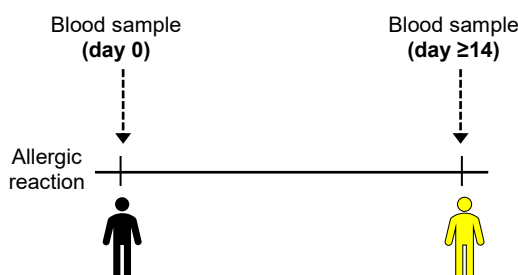
344

345

Table 1. Allergic reactions

Allergic patients	
Number	59
Age (years, SD)	38.7 ± 19.2
Sex (♀)	61%
Trigger of the reaction	
Drugs	69%
Foods	29%
Others	2%
Severity	
Level 1	49%
Level 2	41%
Level 3	10%
Symptoms	
Skin	92%
Mucosal	51%
Airways	36%
Gastrointestinal	20%
Neurologic	12%
Cardiovascular	10%

a



b

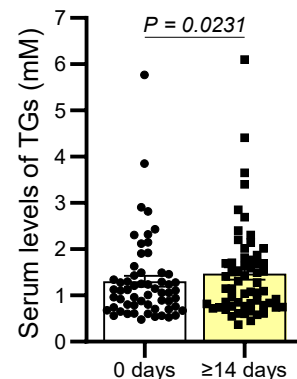


Fig. 7 Allergic patients show increased blood triglyceride (TG) levels days after undergoing an allergic reaction. a Protocol followed for serum collection from 59 allergic patients. **b** Serum TG levels measured at the onset of the allergic reaction and ≥14 days later. Data presented as mean ± s.e.m. Each dot represents an individual patient. Statistically significant differences were calculated with the Wilcoxon rank-sum test.

359 DISCUSSION

360 Recent studies in humans indicate that allergic disease may cause metabolic changes. For example,
 361 it has been reported that children with food allergy have lower serum levels of sphingolipids and
 362 ceramides¹⁷, and severe respiratory allergy has been associated with higher plasma levels of fatty
 363 acids¹⁹. Along the same line, the metabolomic profiling of serum from food allergic children, at the
 364 time of diagnosis and allergy resolution, revealed that the lipid profile is closely related to allergy
 365 outgrowth¹⁸. Also, it has been reported that patients with allergic rhinitis, asthma and atopic dermatitis
 366 have increased risk of dyslipidemia³⁸⁻⁴⁰. While these studies evince the existence of an interplay
 367 between allergic disease and lipid metabolism, the mechanisms involved are poorly understood,
 368 particularly the contribution of the different phases of allergic inflammation to dyslipidemia.

369 Using a murine model of allergy and atherosclerosis, we observed that allergic mice exhibited
 370 dyslipidemia, which was characterized by increased levels of serum TGs. Intriguingly, this serum TG
 371 increase detected in allergic animals was not inherent to allergic disease, but specific to allergic
 372 inflammation. Hence, quiescent allergy or atopy in and of itself did not alter serum TG levels, but an
 373 allergic reaction was required for this to happen. Also, these changes in serum TGs appear to occur
 374 regardless of the diet because the blood was collected under fasting conditions in mice fed
 375 atherosclerosis-prone diets and regular diets. Further studies should determine whether the lipids
 376 released during allergic inflammation, and particularly TGs, are due to *de novo* synthesis in the liver,
 377 local release from adipocytes, and/or to changes in the lipid metabolism of immune cells.

378 Several studies in humans have established a long-lasting association between elevated serum TG
 379 levels and cardiovascular disease⁴¹⁻⁴⁴, although it is still unclear whether TGs promote disease via
 380 direct or indirect mechanisms. A recent study combined large-scale human genetic analysis with
 381 experimental evidence. It showed that TG-lowering alleles involved in hepatic production of TG-rich
 382 lipoproteins (*TM6SF2* and *PNPLA3*) and peripheral lipolysis (*LPL* and *ANGPTL4*) were associated
 383 with lower risk of cardiovascular disease⁴⁵. Also, elevated serum TG levels have been recently
 384 identified as a risk factor of subclinical atherosclerosis in the PESA study, even when the LDL:HDL
 385 ratio was normal²⁵.

386 A number of studies both in rodents^{46,47} and humans^{48,49} have explored metabolic changes following
 387 an allergic reaction, but focusing on the acute phase, to unveil biomarkers or mediators of
 388 anaphylaxis. In other words, these studies analyzed metabolic changes in circulation minutes or
 389 hours after the allergic reaction was triggered. Our comprehensive, untargeted lipidomic analysis in
 390 plasma was performed days (1, 3, and 7) after allergen challenge, well beyond the acute phase
 391 reaction was over. Strikingly, these analyses revealed a unique lipid fingerprint in allergic mice
 392 following an allergic reaction, particularly at 7 days post allergen exposure, as compared to

393 unchallenged allergic mice. Their profile was characterized by an increase in 25 specific TGs, some
 394 of which have been positively associated with risk of cardiovascular disease. For example, the
 395 lipidomic analysis of 685 plasma samples of the prospective population-based Bruneck study found
 396 that TG 56:6, TG 52:2, TG 50:2, and particularly TG 54:2, were significantly associated with
 397 cardiovascular disease risk²⁶. Furthermore, using 5,662 serum lipid profiles from PROMIS (a case-
 398 control study of first-ever acute myocardial infarction), Harshfield *et al.* identified lipids associated
 399 with the genetic polymorphism rs662799 in the *APOA5-APOC3* locus, which is linked to coronary
 400 artery disease. Of these, TG 53:3 and TG 56:4 were positively associated with risk factors of
 401 cardiovascular disease including hypertension and diabetes, respectively²⁸. Also, TG 38:0 has been
 402 identified as a serum biomarker of Wilson's disease, in a cohort of 34 patients that included 34
 403 relatives of these patients and 64 healthy individuals as controls. Wilson's disease is a genetic
 404 pathology characterized by copper accumulation and dysregulated lipid metabolism⁵⁰. Although the
 405 relationship between Wilson's disease and atherosclerosis has not been defined, it has been
 406 reported that Wilson's disease patients are at a higher risk of suffering cardiovascular events⁵¹. On
 407 the other hand, Fernandez *et al.* performed a plasma lipidome using 427 samples from the
 408 prospective population-based Malmö Diet and Cancer (MDC) study. They determined that TG 48:2
 409 was negatively associated with cardiovascular disease²⁷. While further validation of these TG
 410 species is required in well-characterized cohorts of allergic patients, it is noteworthy that a substantial
 411 number of the TG species identified in the murine model have been associated with risk of
 412 cardiovascular disease in humans.

413 To better understand the interplay between allergic disease and lipid metabolism, we took different
 414 approaches to ascertain the contribution of cellular and humoral inflammation to serum TG changes.
 415 Given that the TG peak in serum was observed between 3- and 7-days post-allergen exposure, and
 416 the lipid profile was unique 7 days after the allergic reaction, we considered that these changes were
 417 associated with late phase inflammation, which peaks 3 days after challenge in this model⁵².
 418 Although different players such as type 2 innate lymphoid cells can contribute to late phase
 419 inflammation⁵³, CD4 Th2 cells orchestrate it¹⁶. Surprisingly, the impairment of CD4-T-cell-driven late-
 420 phase inflammation did not affect the increase in serum TG changes, thus pointing towards the acute
 421 phase response. Indeed, using models of passive sensitization, where there is no type 2 adaptive
 422 immune response established, but exclusively the humoral components transferred, we
 423 demonstrated that the acute phase alone was sufficient to recapitulate the increase in serum TGs.
 424 Furthermore, we delved into the role of the classical (IgE-mediated) and alternative (IgG-mediated)
 425 pathways of anaphylaxis to dyslipidemia. Strikingly, the classical pathway of anaphylaxis appeared
 426 to be dispensable for the changes in serum TGs, as these were only observed when the alternative

427 pathway or both were active. Also, the alternative pathway was sufficient to induce a unique lipid
428 signature, clearly different from the one produced by the classical pathway, which was similar to that
429 of the control group. The identification of lipid species that are specifically upregulated days after the
430 onset of an IgG-mediated reaction may be helpful to appraise its actual contribution to human
431 anaphylaxis, which still lacks specific biomarkers¹⁴.

432 From a broader perspective, these data display a novel role for humoral responses, in particular
433 those of the IgG isotype insofar as they can regulate the lipid metabolism in response to allergens.
434 However, it is plausible to consider that this mechanism may operate in other diseases, not
435 necessarily type 2 driven, where strong IgG responses are chronically induced⁵⁴. For example,
436 autoimmune diseases, such systemic lupus erythematosus and rheumatoid arthritis, are associated
437 with dyslipidemia and high serum TG levels, even in patients naive to corticosteroids⁵⁵⁻⁵⁷.

438 Assessing the precise contribution of acute vs late allergic inflammation to serum TG levels in
439 humans is almost an unsurmountable challenge. Even so, we attained to show in a group of 59
440 patients that an allergic reaction induced an increase in serum TG levels days after the reaction. A
441 recent transcriptomic study in blood of 3,229 individuals from the BIOS (Biobank-based Integrative
442 Omics Study) consortium found an association between TG levels and canonical genes of type 2
443 immunity²¹. Although information pertaining to allergic disease of these patients was not available,
444 they found that TG levels were associated with a downregulation of the hallmark Th2 cytokine, *IL4*,
445 two IgE-receptor genes (*FCER1A* and *MS4A2*) as well as genes related to allergic mediators or its
446 metabolism (*HDC*, *HRH4*, *CPA3*, *HPGDS*, *CYP11A1*, *PTGER3*)²¹. In this context, one may speculate
447 that the increase of TGs observed following an allergic reaction is the output of a regulatory
448 mechanism that prevents immunopathology by reducing the expression of key molecules of the
449 allergic machinery. Yet, the chronic use of this putative mechanism of control may be at the cost of
450 a higher risk of developing cardiovascular events.

451

452 EXPERIMENTAL PROCEDURES

453 **Mice.** Age-, sex-, and strain-matched controls were used in all the experiments. B6;129S7-
454 *Ldlrtm1Her/J* mice were crossed with B6.SJL-Ptprc^aPepc^b/BoyCrl mice and selected by genotype
455 (LDLr KO) at CNIC's Animal facility. Mice were maintained in biohazard specific pathogen-free
456 conditions on a 12-hour light-dark cycle with a chow diet (RE; LASQCdiet Rod18-A, Altromin) or a
457 HC diet (SSNIFF, S9167-E010) and water *ad libitum*. All procedures were approved by the
458 Environmental Council of the Community of Madrid (Madrid, Spain) with PROEX references 45.2/20
459 and 9.7/23.

460 **Allergy model.** Male mice were sensitized with 4 mg of PN butter (~1 mg of protein; Capitán Mani)
 461 and 5 µg of cholera toxin (C8052, Sigma) in 0.5 mL of PBS administered intragastrically, weekly for
 462 4 weeks. Following sensitization, mice were challenged intraperitoneally with 2.5 mg of crude peanut
 463 extract (CPE; XPF171D3A25; Stallergens Greer), or 88 µg of CPE per gram of body weight, and
 464 core temperature was assessed rectally with a dual thermometer (620-2049, VWR). Serum or
 465 plasma samples were collected at different times of allergic pathology under 12-16 hours of fasting
 466 and stored at -80°C for further analyses. In some instances, at 3- or 7-days post-allergen challenge,
 467 peritoneal lavage was performed with ice-cold 10 mM EDTA in PBS and spleens were processed to
 468 assess eosinophilia and CD4 T-cell depletion by flow cytometry²³.

469 **Antigen-specific Ig ELISA.** ELISAs were performed in a 96-well flat bottom polystyrene plate (3590,
 470 Corning). Plates were washed with 0.05% Tween-20 in PBS (washing buffer), and 10% FBS/1%
 471 BSA in washing buffer was used as blocking solution. Plates were developed with 50 µl TMB
 472 (421101, BioLegend) and stopped using 50 µl 1.5 N H₂SO₄. Plates were read at 450 nm using a
 473 Thermo Scientific Multiskan FC. No-sample controls were included in all assays. The average optical
 474 density of the no-sample control wells was subtracted from all samples prior to plotting.

475 To determine the serum levels of PN-specific IgE, plates were coated with 50 µl of 2 µg/ml anti-
 476 mouse IgE (clone R35-72M; 553413, BD) in PBS, sealed with aluminum foil, and incubated overnight
 477 at 4°C. The next day, plates were washed and blocked for 2 hours at room temperature (RT). Plates
 478 were washed and incubated with 50 µl of serum diluted to the indicated concentrations in blocking
 479 solution overnight at 4°C. A standard curve was included of purified mouse IgE k Isotype control
 480 (557079, BD Biosciences) from 120 ng/ml to 0.9 ng/ml diluted in PBS. The next day, plates were
 481 washed and incubated with 50 µl of biotinylated-CPE at 150 ng/ml while standards were incubated
 482 with 50 µl of blocking solution, for 90 minutes at RT. Plates were washed and the samples were
 483 incubated with 50 µl of streptavidin-HRP diluted in blocking solution and standards with 50 µl of 0.175
 484 µg/ml rat anti-mouse IgE-HRP (1130-05, Southern Biotech) diluted in blocking solution for 1 hour at
 485 RT. Lastly, plates were washed, developed, stopped, and read.

486 To determine the serum levels of PN-specific IgG1, plates were coated with 10 µg/ml CPE in 50 µl
 487 of carbonate bicarbonate buffer, sealed with aluminum foil, and incubated overnight at 4°C. The next
 488 day, plates were washed and blocked for 2 hours at RT. Plates were washed and incubated with 50
 489 µl of serum diluted to the indicated concentrations in blocking solution overnight at 4°C. The next
 490 day, plates were washed and incubated with 50 µl of 0.5 µg/ml goat anti-mouse IgG1-HRP (A10551,
 491 Thermo Fisher Scientific) in blocking solution for 2 hours at RT. Ultimately, plates were washed,
 492 developed, stopped, and read.

Antibody treatments and passive sensitization. CD4 T-cell depletion was accomplished via 2 intraperitoneal (i.p.) administrations of 200 µg of anti-CD4 (clone GK1.5; BE0003, BioXCell) one week and one day before challenge²². IgG from rat serum (I4131, Sigma-Aldrich) was used as isotype control. Cell depletion was confirmed by flow cytometry.

For passive sensitization, a pool of sera collected from PN-allergic or non-allergic mice under fasting conditions was administered to male naive LDLr KO mice via i.p. injection. For IgG-passive sensitization, part of the PN-allergic sera pool was heated at 57°C for 4 hours to accomplish IgE denaturation^{30,31}. Then, 700 µl of heat-treated sera was transferred to naive recipients the previous day to challenge. The irreversible denaturation and deactivation of IgE was confirmed by ELISA and mast cell activation test³². In the rest of the groups (naive, IgE, and IgE+IgG), the naive or native allergic sera, respectively, were serially transferred as follows: 100 µL; 200 µL; and 400 µL with an interval of 48 hours between each administration. Then, the mice were challenged either the day after the last administration, to induce IgE- and IgG-mediated anaphylaxis, or 10 days later to allow for IgG clearance and IgE-mediated anaphylaxis⁵⁸.

Flow cytometry. Staining was conducted in FACS buffer (2.5 mM EDTA, 0.5% BSA, in PBS) in a 96 well V- or U-bottom plate (Corning, 353077) with combinations of the antibodies described in **Table S3** and the dilutions they were used at, based on 50 µl final staining volume. In all assays, cells were incubated with anti-FcγRII/III (clone 93; 101302, BioLegend) before incubation with fluorochrome-conjugated antibodies. Dead cells were excluded by fixable viability dye eFluor780 (65-0865-18, eBioscience) and gated on singlets. On average, a minimum of 50,000 live and singlet cells were analyzed. Fluorescence minus one (FMO) and unstained controls were used for gating. Data were acquired on a LSR II or Fortessa (BD) and analyzed using FlowJo (FlowJo LLC, Ashland, USA).

Blood lipid profile. Murine serum samples were analyzed with the automated Dimension® RxL Max® clinical chemistry system from Siemens at the Comparative Medicine Unit of CNIC. The assay was performed using a Flex® reagent cartridge. The analysis of the lipid profile included reagents from Siemens (HDL, DF48B; Cholesterol DF27; DF131, LDL; DF55A, Lipase; DF69A, TGs), Spinreact (41035, Free Cholesterol), and Wako (436-91995, 436-91995; NEFA).

Lipidomics. Data acquisition and analysis was performed at CEMBIO and CBQF. Common reagents include reverse-osmosed ultrapure water from Millipore; LC-MS grade methanol (MeOH), acetonitrile (ACN), isopropanol (IPA) and sodium hydroxide from Fisher Scientific, Honeywell or VWR; HPLC grade methyl tert-butyl ether (MTBE), chloroform, ammonium fluoride (NH₄F) (ACS reagent, ≥ 98%) and ammonium formate from Sigma-Aldrich or VWR. Analytical grade ammonia

526 solution (28%, GPR RECTAPUR®) and acetic acid glacial (AnalaR® NORMAPUR®) were obtained
527 from VWR Chemicals.

528 Lipidomics at CEMBIO. Lipid extraction was performed as reported⁵⁹. In brief, 50 µl of plasma from
529 63 mice were thawed on ice for approximately 1 hour and vortexed for 2 min. Subsequently, 800 µl
530 of a previously prepared mixture consisting of MeOH:MTBE:Chloroform (1.33:1:1, v/v/v) and 25 µl
531 light Splash Lipidomics (Mass Spec Standard, 330707, Avanti Polar Lipids, Inc.) used as the internal
532 standard were added to each sample at RT for deproteinization and lipid extraction. Then, samples
533 were vortex-mixed for 5 min at RT and centrifuged for 15 min at 15°C and 16,100 x g. Finally,
534 supernatants were transferred to chromatography vials with inserts and were directly injected into
535 the LC-MS system. In addition, QC samples were set in parallel to the sample preparation. The QC
536 was prepared by pooling equal volumes (30 µl) of each supernatant sample from the study. The QC
537 was split into 5 vials, and these were analyzed throughout the analysis process.

538 Data were acquired using an Agilent 1290 Infinity II UHPLC system coupled to an Agilent 6545
539 quadrupole time-of-flight (QTOF) mass spectrometer. The Agilent 1290 Infinity II Multisampler
540 system, equipped with a multi-wash option, was used to uptake 1 and 2 µl of extracted samples in
541 positive and negative ionization modes, respectively. The multisampler was maintained at 15°C to
542 preserve lipids in a stable environment and avoid precipitation. An Agilent InfinityLab Poroshell 120
543 ECsingle bondC18 (3.0 × 100 mm, 2.7 µm) (Agilent Technologies) column and a compatible guard
544 column (Agilent InfinityLab Poroshell 120 ECsingle bondC18, 3.0 × 5 mm, 2.7 µm) were used and
545 maintained at 50°C. The chromatography gradient started at 70% of B at 0 – 1 min, 86% at 3.5 – 10
546 min, 100% B at 11–17 min. The starting conditions were recovered by min 17, followed by a 2 min
547 re-equilibration time; the total running time was 19 min. The mobile phases used for both positive
548 and negative ionization modes consisted of (A) 10 mM ammonium acetate, 0.2 mM NH₄F in 9:1
549 water/MeOH and (B) 10 mM ammonium acetate, 0.2 mM NH₄F in 2:3:5 ACN/MeOH/IPA. The flow
550 rate was held constant, set at 0.6 ml/min. The multi-wash strategy consisted of a mixture of
551 MeOH:IPA (50:50, v/v) with the wash time set at 15 s, and aqueous phase:organic phase (30:70,
552 v/v) mixture to assist in the starting conditions.

553 The Agilent 6545 QTOF mass spectrometer equipped with a dual AJS ESI ion source was set with
554 the following parameters: 150 V fragmentor, 65 V skimmer, 3500 V capillary voltage, 750 V octopole
555 radio frequency voltage, 10 L/min nebulizer gas flow, 200°C gas temperature, 50 psi nebulizer gas
556 pressure, 12 L/min sheath gas flow, and 300°C sheath gas temperature. Data were collected in
557 centroid in mode positive and negative ESI modes in separate runs, operated in full scan mode from
558 50 to 1700 *m/z* with a scan rate of 3 spectra/s. A solution consisting of two reference mass

559 compounds was used throughout the whole analysis: purine ($C_5H_4N_4$) at m/z 121.0509 for the
 560 positive and m/z 119.0363 for the negative ionization modes; and HP-0921 ($C_{18}H_{18}O_6N_3P_3F_{24}$) at m/z
 561 922.0098 for the positive and m/z 980.0163 (HP-0921+acetate) for the negative ionization modes.
 562 These masses were continuously infused into the system through an Agilent 1260 Iso Pump at a 1
 563 mL/min (split ratio 1:100) to provide a constant mass correction. Ten Iterative-MS/MS runs were
 564 performed for both ion modes at the end of the analytical run. They were operated with an MS and
 565 MS/MS scan rates of 3 spectra/s, 40–1700 m/z mass window, a narrow (~ 1.3 amu) MS/MS isolation
 566 width, 3 precursors per cycle, 5,000 counts, and 0.001% of MS/MS threshold. Five iterative-MS/MS
 567 runs were set with a collision energy of 20 eV, and the subsequent five runs were performed at 40
 568 eV. References masses and contaminants detected in blank samples were excluded from the
 569 analysis to avoid inclusion in the iterative-MS/MS.

570 The data collected after the LC-MS analyses in both positive and negative ion modes were
 571 reprocessed with the Agilent MassHunter Profinder B.10.0.2 software. The datasets were extracted
 572 using the Batch Recursive Feature Extraction (RFE) workflow integrated into the software. This
 573 workflow comprises two steps: the Batch Molecular Feature Extraction (MFE) and the Batch Find by
 574 Ion Feature extraction (Fbl). The MFE algorithm consists in removing unwanted information,
 575 including the background noise, and then creating a list of possible components that represent the
 576 full range of TOF mass spectral data features, which are the sum of coeluting ions that are related
 577 by charge-state envelope, isotope pattern, and/or the presence of different adducts and dimers.
 578 Additionally, the MFE is intended to detect coeluting adducts of the same feature, selecting the
 579 following adducts: $[M+H]^+$, $[M+Na]^+$, $[M+K]^+$, $[M+NH_4]^+$ and $[M+C_2H_6N_2+H]^+$ in LC-MS positive
 580 ionization; $[M-H]^-$, $[M+CH_3COOH-H]^-$, and $[M+Cl]^-$ in LC-MS negative ion mode. The neutral loss
 581 (NL) of water is also considered for both ion modes. The algorithm then aligns the molecular features
 582 across the study samples using the mass and retention time to build a single spectrum for each
 583 compound group. The next step involves Fbl, using the median values derived from the MFE process
 584 to perform a targeted extraction to improve the reliability of finding and reporting features from
 585 complex datasets used for differential analysis.

586 After data pre-processing, quality assurance (QA) consisted of raw data filtration by keeping all
 587 features that were present after blank subtraction, were detected in >50% of QCs and >75% in at
 588 least one sample group and had Relative Standard Deviation (RSD) <30% in the QCs. The rest of
 589 the signals were excluded from the analyses. Finally, 1,106 and 268 chemical entities were obtained
 590 that passed LC-MS quality control in positive and negative ionization, respectively. Missing values
 591 were replaced using the k-nearest neighbors (kNN) algorithm⁶⁰ using an in-house script developed
 592 in Matlab® (v.R2018b, MathWorks®). The quality of the analyses was tested using PCA models⁶¹.

593 The lipid annotation process was carried out in three steps: the first one was an initial tentative
594 identification of lipid features, based on the MS1 data, using our online tool CEU Mass Mediator
595 (CMM) (<http://ceumass.eps.uspceu.es/mediator/>)⁶². This tool for mass-based compound annotation
596 comprises the information available in different databases (KEGG, HMDB, LIPID MAPS, Metlin,
597 MINE and an in-house library). This stage started with the tentative assignment based on (i) accurate
598 mass (maximum mass error tolerance 20 ppm); (ii) retention time; (iii) isotopic pattern distribution;
599 (iv) the possibility of cation and anion formation; and (v) adduct formation pattern.

600 Secondly, to increase the level of confidence annotation, the raw LC-MS/MS data obtained was
601 imported to the Lipid Annotator software (Agilent Technologies Inc.) and the MS-DIAL software⁶³, to
602 build a fragmentation-based (MS/MS) library comprising the *m/z* of all the precursors identified as
603 lipids by the software, together with their corresponding RT. The Lipid Annotator method⁶⁴ was set
604 as follows: ion species $[M+H]^+$, $[M+Na]^+$, and $[M+NH_4]^+$ for positive; and $[M-H]^-$, and $[M+CH_3COOH-$
605 $H]^-$ for negative ionization mode. Then, for both ion modes, the Q-Score was set at ≥ 50 ; all the lipid
606 classes were selected, the mass deviation was established as ≤ 20 ppm, fragment score threshold
607 was fixed as ≥ 30 , and the total score was set at ≥ 60 . For the case of MS-DIAL software, analytical
608 parameters were also set as described: ion species $[M+H]^+$, $[M-H_2O+H]^+$, $[M+Na]^+$, $[M+K]^+$,
609 $[M+NH_4]^+$ and $[M+C_2H_6N_2+H]^+$ for positive; and $[M-H]^-$, $[M-H_2O-H]^-$, $[M+Cl]^-$, $[M+HCOOH-H]^-$ and
610 $[M+CH_3COOH-H]^-$ for negative mode. Adduct formation with formic acid were observed
611 experimentally in this study even though the mobile phases used for LC are lacking this compound.
612 Formic acid presence was considered due to trace amount contamination levels of formate in acetate
613 salts of LC-MS grade, or MeOH oxidation during ESI. The search was fixed to be performed across
614 a mass range from 50 to 1500 Da (for both MS1 and MS/MS levels), the mass deviation accepted
615 was ≤ 0.01 Da and ≤ 0.025 for MS1 and MS/MS levels respectively, and the identification score cut
616 off was also set at ≥ 60 .

617 Finally, a manual MS/MS spectral interpretation was carried out using the software Agilent
618 MassHunter (version 10.0), matching the retention time and MS/MS fragmentation to the available
619 spectral data included in MetFrag and Lipid Maps⁶⁵. Different forms of cations and anions were
620 targeted for the same molecule to ensure its annotations. The interpretation of each obtained
621 spectrum led to the same ID in terms of belonging to the same lipid category and in terms of fatty
622 acids composition, which together give a robust and complete identification. The nomenclature used
623 in this article for the lipid species reported follows the latest update of the shorthand annotation.⁶⁶
624 Lipid metabolic networks according to their chain length, saturation, and level of significance were
625 performed by version 1 LINEX webapp.

626 Lipidomics at CBQF. Lipid extraction from 20 plasma samples was performed as reported⁶⁷ with
627 some modifications. Briefly, tubes were added with 1.5 mL of MeOH and 5 mL of MTBE. Samples
628 were homogenized for 1 min followed by 15 min of sonication in ultrasound. This procedure was
629 repeated once again and then the tubes let under rotation (70 rpm) overnight (18 h). Afterward, tubes
630 were added with 1.25 mL of HPLC-water, homogenized for 1 min and centrifuged (1250 x g, 10 min,
631 room temperature). About 3 mL of the upper layer (MTBE containing the extracted lipids) were
632 recovered to a new tube previously weighted. Then, 3 mL of MTBE were added to extraction tubes
633 and these homogenized and centrifuged at the same above-mentioned conditions. Upper layer was
634 recovered, and the MTBE extract let to evaporate completely, under nitrogen, for further
635 determination of lipid extract mass.

636 Plasma lipid extracts were pooled according to their group, dissolved in IPA:ACN (9:1, v/v) at 0.2
637 mg/mL and analyzed in triplicate on an UHPLC instrument (Elute; Bruker), equipped with an Acquity
638 UPLC BEH C18 (17 μ m) pre-column (Waters), an Intensity Solo 2 C18 (100 x 2.1 mm) column
639 (Bruker), and coupled with an UHR-QTOF detector (Impact II; Bruker). The injection method was
640 based on conditions previously reported with some modifications⁶⁸. Thus, mobile phases consisted
641 of ACN:upH₂O (6:4, v/v) (Phase A) and IPA:ACN (9:1, v/v) (Phase B), each one added with 0.1%
642 (v/v) formic acid and 10 mM ammonium formate. Phase B gradient flow was set as follows: 0.0 min:
643 40%, 2.0 min: 43%, 2.1 min: 50%, 12.0 min: 54%, 12.1 min: 70%, 18.0 min: 99%, 20.0 min: 99%,
644 20.1 min: 40%, and 22 min: 40%. Flow rate was set at 0.4 mL/min and column temperature at 55
645 °C. The injection volume was 3 μ L in positive ionization mode and 5 μ L in negative ionization mode.
646 For MS analysis, the following parameters were applied: end plate offset voltage 500 V, capillary
647 voltage 4500 V (positive ionization) or 3000 V (negative ionization), nebulizing gas pressure 35 psi,
648 drying gas flow 8 L/min, drying gas temperature 325 °C, quadrupole ion energy 3 eV (positive
649 ionization) or 5 eV (negative ionization), collision energy 10 eV (positive ionization) or 5 eV (negative
650 ionization). Acquisition was performed in an auto MS/MS scan mode over a mass range of m/z 50-
651 1500. For both ionization modes, an external mass calibration was performed with a solution of
652 IPA:upH₂O (1:1, v/v) added with 0.2% (v/v) formic acid and 0.6% (v/v) NaOH 1M, continuously
653 injected at 180 μ L/h.

654 The files resulted from LC-ESI-QTOF analysis were converted into abf format through Reifycs
655 Analysis Base File Converter (Reifycs Inc.). These converted files were used for lipid composition
656 analysis in MS-Dial 5.1.230517 (Riken). The alignment results were exported and identified
657 compounds were grouped by lipid class, according to LIPID MAPS database nomenclature. Peak
658 intensities of compounds belonging to same lipid class were totalized and used as data for heatmap
659 analysis in ClustVis, a web tool available for visualizing clustering of multivariate data⁶⁹. The MSDial

software was able to detect 2,718 different ions among the serum samples, being identified 1,236 compounds by the software. From these data was excluded, among the compounds with attributed equal identification, the ones that revealed considerably low signal, leading to a total of 1,198 compounds to assess further statistical analysis. For heatmap analysis, compounds were grouped into 36 lipid classes.

665

TG measurements in human sera. Human TGs were measured using the Cobas c 501 analyzer (Roche Diagnostic). For this purpose, serum samples (BD Vacutainer tubes) were collected from each patient under two conditions: one during the onset of a hypersensitivity reaction and the other at least 14 days after the reaction. If the allergic reaction occurred accidentally, the first samples were collected in the emergency departments, whereas if it was due to a controlled challenge test, the sera were obtained in the allergy units.

Study population included 118 paired sera from 59 patients presenting hypersensitivity reactions and recruited from three Spanish hospitals (Hospital Universitario Fundación Jiménez Díaz, Hospital Central de la Cruz Roja, Hospital Infantil Universitario Niño Jesús). Each patient's sex, age, reaction trigger, clinical signs and symptoms were recorded. In addition, the severity of the reaction was determined according to the criteria established by Brown³⁶. The study was approved by the Ethics Committee (CEIm FJD, PIC057-19), and authors adhered to the declaration of Helsinki. All patients were included after giving informed consent by the donors or their parents. Inclusion criteria included acceptance to participate in the study and an objective diagnosis of the reaction. Exclusion criteria were the presence of a blood-borne disease, any psychiatric illness or psychological pathology that prevented acceptance for the study or receiving any treatment prior to obtaining the acute phase sample, as these interfere with TG levels.

683

Statistics. Independent experiments were performed with multiple biological replicates to ensure reproducibility and statistical power to detect meaningful differences. GraphPad Prism v9 was used for all statistical analyses. Quantitative variables are expressed as means \pm standard error of the mean (s.e.m.). Normal distribution was determined by D'Agostino and Pearson test, Shapiro–Wilk test, Kolmogorov–Smirnov test, and Anderson–Darling test. A two-way analysis of variance (ANOVA) or mixed-effects test were used to evaluate differences between more than two groups with a parametric distribution, and Bonferroni's multiple comparison test was applied. Data with nonparametric distribution were evaluated with the Kruskal–Wallis test for more than two groups, and the Mann–Whitney or Wilcoxon signed-rank test for two independent groups. A p-value<0.05 was considered significant.

694 For lipidomic data, multivariate analysis was performed using SIMCA v.16.0 (Sartorius Stedim Data
695 Analytics). The PCA models were used to evaluate data quality and find patterns in the experimental
696 samples. The models were unit variance scaled and evaluated using R^2 and Q^2 parameters, which
697 are the classification and prediction capacity, respectively. Complementary, univariate analysis was
698 performed in MATLAB (v.R2018b, MathWorks®) or with the Lipidmaps' statistical tool to obtain the
699 significance of each feature in the study. The focus was set on the comparison between two groups
700 at day 7. For this statistical analysis, T-test student or Mann-Whitney U test was applied for each
701 metabolite, depending on the normality of the data, which were evaluated by the Kolmogorow-
702 Smirnow-Lilliefors test and the Levene test, respectively. The FDR was performed by using the
703 Benjamini-Hochberg correction for these p-values, and statistical significance was set at 95% level
704 ($pFDR < 0.05$ for the adjusted p-value)⁷⁰. The MetaboAnalyst online tool (v. 5.0) was used to produce
705 heat maps with hierarchical clustering. Euclidean distance measure and Ward's clustering method
706 were chosen as the clustering parameters. For lipid maps, LINEX – LipidNetworkExplorer online tool
707 was used (<https://exbio.wzw.tum.de/linex>). GraphPad Prism v9 was used to represent plots with
708 metabolomics data.

709

710 **AUTHOR CONTRIBUTIONS.** N.F.-G, R.C.-G. and R.J.-S. performed the *in vivo* experiments and
711 analyzed the data. L.M.-S. did ELISAs. A.J.G.-C., A.G., D.O., L.M.-S, A.L.-F. and L.L.-P. performed
712 lipidomics, and L.M.R.-A., A.V., D.B., and C.Barbas provided supervision and aided in lipidomics
713 data processing. E.S.-M. and C.L.-S. conducted mast cell cultures and activation assays. M.R.-H.
714 and I.R.-F. helped with experiments. E.N.-B., V.E., and C.Blanco provided samples from allergic
715 patients and/or measured their lipid profile. Y.R.C., B.I., P.M. and F.S.-M. provided expertise in
716 immunology and/or atherosclerosis throughout the project. R.J.-S conceptualized and oversaw the
717 project, designed experiments, and wrote the manuscript. All authors discussed the results, assisted
718 in the preparation of the manuscript, and approved its publication.

719 **COMPETING INTERESTS:** The authors declare no competing interests.

720 **ACKNOWLEDGEMENTS.** R.J.-S.'s laboratory has received support from the Severo Ochoa
721 Program (AEI/SEV-2017- 0712; Spain), FSE/FEDER through the Instituto de Salud Carlos III (ISCIII;
722 CP20/00043; PI22/00236; Spain), The Nutricia Research Foundation (NRF-2021-13; The
723 Netherlands), New Frontiers in Research Fund (NFRFE-2019-00083; Canada) and SEAIC
724 (BECA20A9; Spain). F.S.-M. reports grants from Ministerio de Ciencia e Innovación (MICIN;
725 PID2020-120412RB-I00; Spain), and Comunidad de Madrid (INTEGRAMUNE, P2022/BMD7209;
726 Spain). V.E. obtained support from the ISCIII (PI21/00158; Spain). N.F.-G. and I.R.-F. received a

727 Formación de Profesorado Universitario grant (FPU16/03953 and FPU20/05176, respectively) from
 728 Ministerio de Universidades (Spain). N.F.-G. and L.M.-S. are supported by the INVESTIGO Program
 729 of the Comunidad de Madrid and Ministerio de Trabajo y Economía Social, Servicio Público de
 730 Empleo (SEPE), respectively, which is funded by “Plan de Recuperación, Transformación y
 731 Resiliencia” and “NextGenerationEU” of the European Union (09-PIN1-00015.6/2022 and 2022-
 732 C23.I01.P03.S0020-0000031). R.C.-G. is supported by Ayudas para contratos Juan de la Cierva-
 733 formación 2021 (FJC2021-047282-I) from MICIN (Spain). P.M. is supported by MICIN-ISCIII-Fondo
 734 de Investigación Sanitaria (PI22/01759; PMPTA22/00090-BIOCARDIOTOX) and Comunidad de
 735 Madrid (P2022/BMD-7209-INTEGRAMUNE-CM; Spain). The CNIC is supported by the ISCIII, the
 736 MICIN, and the Pro CNIC Foundation. CNIC is a Severo Ochoa Center of Excellence (grant
 737 CEX2020-001041-S funded by MICIN/AEI/10.13039/501100011033). The R.J.-S.’s lab recognizes
 738 Ana Cayuela, Ibon Redondo, Pedro L. Majano, Francisco Vega, María Ángeles Vallejo, Melissa
 739 Gordon, María Jesús Andrés and all the members of the R.J.-S. and F.S.-M. labs for technical help
 740 and/or scientific input.

741

742 REFERENCES

- 743 1 Molofsky, A. B. & Locksley, R. M. The ins and outs of innate and adaptive type 2
 744 immunity. *Immunity* **56**, 704-722 (2023). <https://doi.org/10.1016/j.immuni.2023.03.014>
- 745 2 Gause, W. C., Rothlin, C. & Loke, P. n. Heterogeneity in the initiation, development and
 746 function of type 2 immunity. *Nature Reviews Immunology* **20**, 603-614 (2020).
 747 <https://doi.org/10.1038/s41577-020-0301-x>
- 748 3 Kopp, E. B., Agaronyan, K., Licona-Limón, I., Nish, S. A. & Medzhitov, R. Modes of type
 749 2 immune response initiation. *Immunity* **56**, 687-694 (2023).
 750 <https://doi.org/10.1016/j.immuni.2023.03.015>
- 751 4 Akdis, C. A. Does the epithelial barrier hypothesis explain the increase in allergy,
 752 autoimmunity and other chronic conditions? *Nature Reviews Immunology* **21**, 739-751
 753 (2021). <https://doi.org/10.1038/s41577-021-00538-7>
- 754 5 Knoflach, M. *et al.* Allergic Rhinitis, Asthma, and Atherosclerosis in the Bruneck and
 755 ARMY Studies. *Archives of Internal Medicine* **165**, 2521-2526 (2005).
 756 <https://doi.org/10.1001/archinte.165.21.2521>
- 757 6 Wilson, J. M. *et al.* IgE to the Mammalian Oligosaccharide Galactose- α -1,3-Galactose Is
 758 Associated With Increased Atheroma Volume and Plaques With Unstable
 759 Characteristics—Brief Report. *Arteriosclerosis, Thrombosis, and Vascular Biology* **38**,
 760 1665-1669 (2018). <https://doi.org/10.1161/atvbaha.118.311222>
- 761 7 Roth, G. A. *et al.* Global Burden of Cardiovascular Diseases and Risk Factors, 1990–
 762 2019. *Journal of the American College of Cardiology* **76**, 2982-3021 (2020).
 763 <https://doi.org/10.1016/j.jacc.2020.11.010>
- 764 8 Libby, P. *et al.* Atherosclerosis. *Nature Reviews Disease Primers* **5**, 56 (2019).
 765 <https://doi.org/10.1038/s41572-019-0106-z>

- 9 Björkegren, J. L. M. & Lusis, A. J. Atherosclerosis: Recent developments. *Cell* **185**, 1630-1645 (2022). <https://doi.org/10.1016/j.cell.2022.04.004>
- 10 Fernández-Gallego, N. *et al.* The impact of type 2 immunity and allergic diseases in atherosclerosis. *Allergy* **77**, 3249-3266 (2022). <https://doi.org/10.1111/all.15426>
- 11 Wang, H. *et al.* Global, regional, and national life expectancy, all-cause mortality, and cause-specific mortality for 249 causes of death, 1980–2015: a systematic analysis for the Global Burden of Disease Study 2015. *The Lancet* **388**, 1459-1544 (2016). [https://doi.org/10.1016/s0140-6736\(16\)31012-1](https://doi.org/10.1016/s0140-6736(16)31012-1)
- 12 Townsend, N. *et al.* Epidemiology of cardiovascular disease in Europe. *Nature Reviews Cardiology* **19**, 133-143 (2021). <https://doi.org/10.1038/s41569-021-00607-3>
- 13 Galli, S. J. & Tsai, M. IgE and mast cells in allergic disease. *Nature Medicine* **18**, 693-704 (2012). <https://doi.org/10.1038/nm.2755>
- 14 Finkelman, F. D., Khodoun, M. V. & Strait, R. Human IgE-independent systemic anaphylaxis. *Journal of Allergy and Clinical Immunology* **137**, 1674-1680 (2016). <https://doi.org/10.1016/j.jaci.2016.02.015>
- 15 Jönsson, F. *et al.* An IgG-induced neutrophil activation pathway contributes to human drug-induced anaphylaxis. *Science Translational Medicine* **11**, eaat1479 (2019). <https://doi.org/10.1126/scitranslmed.aat1479>
- 16 Galli, S. J., Tsai, M. & Piliponsky, A. M. The development of allergic inflammation. *Nature* **454**, 445-454 (2008). <https://doi.org/10.1038/nature07204>
- 17 Crestani, E. *et al.* Untargeted metabolomic profiling identifies disease-specific signatures in food allergy and asthma. *Journal of Allergy and Clinical Immunology* **145**, 897-906 (2020). <https://doi.org/10.1016/j.jaci.2019.10.014>
- 18 Jang, H. *et al.* Metabolomic profiling revealed altered lipid metabolite levels in childhood food allergy. *Journal of Allergy and Clinical Immunology* **149**, 1722-1731.e1729 (2022). <https://doi.org/10.1016/j.jaci.2021.10.034>
- 19 Obeso, D. *et al.* Multi-omics analysis points to altered platelet functions in severe food-associated respiratory allergy. *Allergy* **73**, 2137-2149 (2018). <https://doi.org/10.1111/all.13563>
- 20 Ellul, S. *et al.* Plasma metabolomic profiles associated with infant food allergy with further consideration of other early life factors. *Prostaglandins, Leukotrienes and Essential Fatty Acids* **159**, 102099 (2020). <https://doi.org/10.1016/j.plefa.2020.102099>
- 21 Dekkers, K. F. *et al.* Lipid-induced transcriptomic changes in blood link to lipid metabolism and allergic response. *Nature Communications* **14**, 544 (2023). <https://doi.org/10.1038/s41467-022-35663-x>
- 22 Jiménez-Saiz, R. *et al.* Lifelong memory responses perpetuate humoral T H 2 immunity and anaphylaxis in food allergy. *Journal of Allergy and Clinical Immunology* **140**, 1604-1615.e1605 (2017). <https://doi.org/10.1016/j.jaci.2017.01.018>
- 23 Chu, D. K. *et al.* Indigenous enteric eosinophils control DCs to initiate a primary Th2 immune response in vivo. *Journal of Experimental Medicine* **211**, 1657-1672 (2014). <https://doi.org/10.1084/jem.20131800>
- 24 Ishibashi, S. *et al.* Hypercholesterolemia in low density lipoprotein receptor knockout mice and its reversal by adenovirus-mediated gene delivery. *J. Clin. Invest.* **92**, 883-893 (1993). <https://doi.org/10.1172/jci116663>
- 25 Raposeiras-Roubin, S. *et al.* Triglycerides and Residual Atherosclerotic Risk. *Journal of the American College of Cardiology* **77**, 3031-3041 (2021). <https://doi.org/10.1016/j.jacc.2021.04.059>
- 26 Stegeman, C. *et al.* Lipidomics Profiling and Risk of Cardiovascular Disease in the Prospective Population-Based Bruneck Study. *Circulation* **129**, 1821-1831 (2014). <https://doi.org/10.1161/circulationaha.113.002500>

816 27 Kiechl, S. *et al.* Plasma Lipid Composition and Risk of Developing Cardiovascular
817 Disease. *PLoS ONE* **8**, e71846 (2013). <https://doi.org/10.1371/journal.pone.0071846>
818 28 Harshfield, E. L. *et al.* An Unbiased Lipid Phenotyping Approach To Study the Genetic
819 Determinants of Lipids and Their Association with Coronary Heart Disease Risk Factors.
820 *Journal of Proteome Research* **18**, 2397-2410 (2019).
821 <https://doi.org/10.1021/acs.jproteome.8b00786>
822 29 Bruton, K. *et al.* Interrupting reactivation of immunologic memory diverts the allergic
823 response and prevents anaphylaxis. *Journal of Allergy and Clinical Immunology* **147**,
824 1381-1392 (2021). <https://doi.org/10.1016/j.jaci.2020.11.042>
825 30 Ishizaka, K., Ishizaka, T. & Menzel, A. E. Physicochemical properties of reaginic
826 antibody. VI. Effect of heat on gamma-E-, gamma-G- and gamma-A-antibodies in the
827 sera of ragweed sensitive patients. *J Immunol* **99**, 610-618 (1967).
828 31 Dorrington, K. J. & Bennich, H. Thermally induced structural changes in immunoglobulin
829 E. *J Biol Chem* **248**, 8378-8384 (1973).
830 32 López-Sanz, C., Sánchez-Martínez, E. & Jiménez-Saiz, R. Protocol to desensitize
831 human and murine mast cells after polyclonal IgE sensitization. *STAR Protocols* **3**,
832 101755 (2022). <https://doi.org/10.1016/j.xpro.2022.101755>
833 33 Kubo, S., Nakayama, T., Matsuoka, K., Yonekawa, H. & Karasuyama, H. Long Term
834 Maintenance of IgE-Mediated Memory in Mast Cells in the Absence of Detectable Serum
835 IgE. *The Journal of Immunology* **170**, 775-780 (2003).
836 <https://doi.org/10.4049/jimmunol.170.2.775>
837 34 Martín-López, L. *et al.* Environmental exposure of Der p 23 in household dust samples.
838 *Clinical & Experimental Allergy* **51**, 1645-1647 (2021). <https://doi.org/10.1111/cea.14004>
839 35 Brough, H. A., Mills, E. N. C., Richards, K., Lack, G. & Johnson, P. E. Mass
840 spectrometry confirmation that clinically important peanut protein allergens are present
841 in household dust. *Allergy* **75**, 709-712 (2019). <https://doi.org/10.1111/all.14070>
842 36 Brown, S. G. A. Clinical features and severity grading of anaphylaxis. *Journal of Allergy*
843 *and Clinical Immunology* **114**, 371-376 (2004). <https://doi.org/10.1016/j.jaci.2004.04.029>
844 37 Ettinger, W. H. & Hazzard, W. R. Prednisone increases very low density lipoprotein and
845 high density lipoprotein in healthy men. *Metabolism* **37**, 1055-1058 (1988).
846 [https://doi.org/10.1016/0026-0495\(88\)90067-4](https://doi.org/10.1016/0026-0495(88)90067-4)
847 38 Sheha, D. S., El-Korashi, L. A., AbdAllah, A. M., El-Beghermy, M. M. & Elmahdi, A. R.
848 Dyslipidemia among allergic rhinitis patients: Frequency and risk factors. *World Allergy*
849 *Organization Journal* **14**, 100523 (2021). <https://doi.org/10.1016/j.waojou.2021.100523>
850 39 La Mantia, I., Andaloro, C., Albanese, P. G. & Varricchio, A. Blood lipid levels related to
851 allergic rhinitis: a significant association. *EuroMediterranean Biomed J* **12**, 144-147
852 (2017).
853 40 Rhee, T.-M., Choi, E.-K., Han, K.-D., Lee, S.-R. & Oh, S. Impact of the Combinations of
854 Allergic Diseases on Myocardial Infarction and Mortality. *The Journal of Allergy and*
855 *Clinical Immunology: In Practice* **9**, 872-880.e874 (2021).
856 <https://doi.org/10.1016/j.jaip.2020.09.008>
857 41 Sarwar, N. *et al.* Triglycerides and the Risk of Coronary Heart Disease. *Circulation* **115**,
858 450-458 (2007). <https://doi.org/10.1161/circulationaha.106.637793>
859 42 Austin, M. A., Hokanson, J. E. & Edwards, K. L. Hypertriglyceridemia as a
860 Cardiovascular Risk Factor. *The American Journal of Cardiology* **81**, 7B-12B (1998).
861 [https://doi.org/10.1016/s0002-9149\(98\)00031-9](https://doi.org/10.1016/s0002-9149(98)00031-9)
862 43 Nordestgaard, B. G. & Varbo, A. Triglycerides and cardiovascular disease. *The Lancet*
863 **384**, 626-635 (2014). [https://doi.org/10.1016/s0140-6736\(14\)61177-6](https://doi.org/10.1016/s0140-6736(14)61177-6)
864 44 Klempfner, R. *et al.* Elevated Triglyceride Level Is Independently Associated With
865 Increased All-Cause Mortality in Patients With Established Coronary Heart Disease.

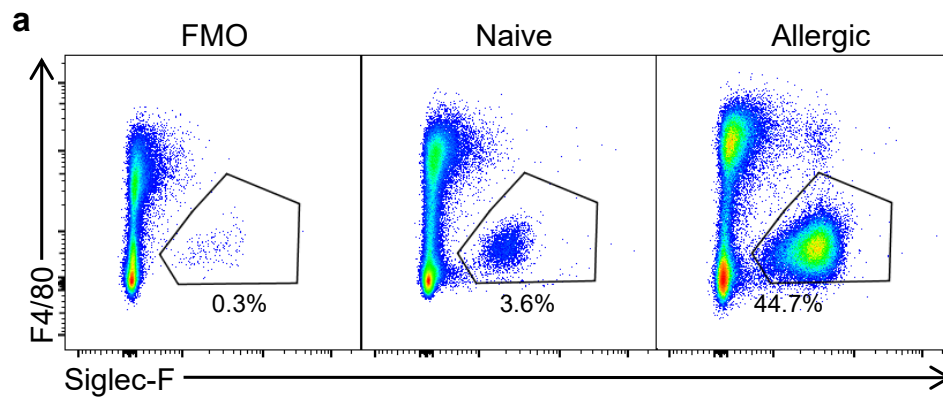
- 866 *Circulation: Cardiovascular Quality and Outcomes* **9**, 100-108 (2016).
867 <https://doi.org/10.1161/circoutcomes.115.002104>
- 868 45 Liu, D. J. *et al.* Exome-wide association study of plasma lipids in >300,000 individuals.
869 *Nature Genetics* **49**, 1758-1766 (2017). <https://doi.org/10.1038/ng.3977>
- 870 46 Xu, Y., Guo, N., Dou, D., Ran, X. & Liu, C. Metabolomics analysis of anaphylactoid
871 reaction reveals its mechanism in a rat model. *Asian Pacific Journal of Allergy and*
872 *Immunology* **35**, 224-232 (2018). <https://doi.org/10.12932/ap0845>
- 873 47 Sun, S. *et al.* Integrating Widely Targeted Lipidomics and Transcriptomics Unravels
874 Aberrant Lipid Metabolism and Identifies Potential Biomarkers of Food Allergies in Rats.
875 *Molecular Nutrition & Food Research* **67**, e2200365 (2023).
876 <https://doi.org/10.1002/mnfr.202200365>
- 877 48 Perales-Chorda, C. *et al.* Characterization of anaphylaxis reveals different metabolic
878 changes depending on severity and triggers. *Clinical & Experimental Allergy* **51**, 1295-
879 1309 (2021). <https://doi.org/10.1111/cea.13991>
- 880 49 Nuñez-Borque, E. *et al.* Proteomic profile of extracellular vesicles in anaphylaxis and
881 their role in vascular permeability. *Allergy* **76**, 2276-2279 (2021).
882 <https://doi.org/10.1111/all.14792>
- 883 50 Zhi, Y. *et al.* HR-MS Based Untargeted Lipidomics Reveals Characteristic Lipid
884 Signatures of Wilson's Disease. *Front Pharmacol* **12**, 754185 (2021).
885 <https://doi.org/10.3389/fphar.2021.754185>
- 886 51 Grandis, D. J. *et al.* Wilson's Disease and Cardiac Myopathy. *The American Journal of*
887 *Cardiology* **120**, 2056-2060 (2017). <https://doi.org/10.1016/j.amjcard.2017.08.025>
- 888 52 Sun, J. *et al.* Impact of CD40 Ligand, B Cells, and Mast Cells in Peanut-Induced
889 Anaphylactic Responses. *The Journal of Immunology* **179**, 6696-6703 (2007).
890 <https://doi.org/10.4049/jimmunol.179.10.6696>
- 891 53 Bartemes, K. R. & Kita, H. Roles of innate lymphoid cells (ILCs) in allergic diseases: The
892 10-year anniversary for ILC2s. *Journal of Allergy and Clinical Immunology* **147**, 1531-
893 1547 (2021). <https://doi.org/10.1016/j.jaci.2021.03.015>
- 894 54 Toms, T. E. Dyslipidaemia in Rheumatological Autoimmune Diseases. *The Open*
895 *Cardiovascular Medicine Journal* **5**, 64-75 (2011).
896 <https://doi.org/10.2174/1874192401105010064>
- 897 55 van Halm, V. P. *et al.* Lipids and inflammation: serial measurements of the lipid profile of
898 blood donors who later developed rheumatoid arthritis. *Annals of the Rheumatic*
899 *Diseases* **66**, 184-188 (2006). <https://doi.org/10.1136/ard.2006.051672>
- 900 56 Rodríguez-Carrio, J. *et al.* High triglycerides and low high-density lipoprotein cholesterol
901 lipid profile in rheumatoid arthritis: A potential link among inflammation, oxidative status,
902 and dysfunctional high-density lipoprotein. *Journal of Clinical Lipidology* **11**, 1043-
903 1054.e1042 (2017). <https://doi.org/10.1016/j.jacl.2017.05.009>
- 904 57 Nuttall, S. L. Cardiovascular risk in systemic lupus erythematosus--evidence of
905 increased oxidative stress and dyslipidaemia. *Rheumatology* **42**, 758-762 (2003).
906 <https://doi.org/10.1093/rheumatology/keg212>
- 907 58 Vieira, P. & Rajewsky, K. The half-lives of serum immunoglobulins in adult mice.
908 *European journal of immunology* **18**, 313-316 (1988).
909 <https://doi.org/10.1002/eji.1830180221>
- 910 59 Gonzalez-Riano, C., Gradillas, A. & Barbas, C. Exploiting the formation of adducts in
911 mobile phases with ammonium fluoride for the enhancement of annotation in liquid
912 chromatography-high resolution mass spectrometry based lipidomics. *Journal of*
913 *Chromatography Open* **1**, 100018 (2021). <https://doi.org/10.1016/j.jcoa.2021.100018>
- 914 60 Armitage, E. G., Godzien, J., Alonso-Herranz, V., López-González, Á. & Barbas, C.
915 Missing value imputation strategies for metabolomics data. *Electrophoresis* **36**, 3050-
916 3060 (2015). <https://doi.org/10.1002/elps.201500352>

- 61 Kellogg, J. J., Kvalheim, O. M. & Cech, N. B. Composite score analysis for unsupervised
comparison and network visualization of metabolomics data. *Analytica Chimica Acta*
1095, 38-47 (2020). <https://doi.org/10.1016/j.aca.2019.10.029>
- 62 Gil de la Fuente, A. *et al.* Knowledge-based metabolite annotation tool: CEU Mass
Mediator. *Journal of Pharmaceutical and Biomedical Analysis* **154**, 138-149 (2018).
<https://doi.org/10.1016/j.jpba.2018.02.046>
- 63 Tsugawa, H. *et al.* MS-DIAL 4: accelerating lipidomics using an MS/MS, CCS, and
retention time atlas. *bioRxiv*, 2020.2002.2011.944900 (2020).
<https://doi.org/10.1101/2020.02.11.944900>
- 64 Koelmel, J. P. *et al.* Lipid Annotator: Towards Accurate Annotation in Non-Targeted
Liquid Chromatography High-Resolution Tandem Mass Spectrometry (LC-HRMS/MS)
Lipidomics Using a Rapid and User-Friendly Software. *Metabolites* **10**, 101 (2020).
<https://doi.org/10.3390/metabo10030101>
- 65 Han, X. *Lipidomics: Comprehensive mass spectrometry of lipids*. (John Wiley & Sons,
2016).
- 66 Liebisch, G. *et al.* Update on LIPID MAPS classification, nomenclature, and shorthand
notation for MS-derived lipid structures. *Journal of lipid research* **61**, 1539-1555 (2020).
<https://doi.org/10.1194/jlr.S120001025>
- 67 Matyash, V., Liebisch, G., Kurzchalia, T. V., Shevchenko, A. & Schwudke, D. Lipid
extraction by methyl-tert-butyl ether for high-throughput lipidomics. *Journal of lipid
research* **49**, 1137-1146 (2008). <https://doi.org/10.1194/jlr.D700041-JLR200>
- 68 Teixeira, F. S. *et al.* Differential Lipid Accumulation on HepG2 Cells Triggered by
Palmitic and Linoleic Fatty Acids Exposure. *Molecules* **28** (2023).
<https://doi.org/10.3390/molecules28052367>
- 69 Metsalu, T. & Vilo, J. ClustVis: a web tool for visualizing clustering of multivariate data
using Principal Component Analysis and heatmap. *Nucleic Acids Research* **43**, W566-
W570 (2015). <https://doi.org/10.1093/nar/gkv468>
- 70 Benjamini, Y., Krieger, A. M. & Yekutieli, D. Adaptive linear step-up procedures that
control the false discovery rate. *Biometrika* **93**, 491-507 (2006).
<https://doi.org/10.1093/biomet/93.3.491>

960

961 **SUPPLEMENTARY FIGURE**

962



963

964 **Fig. S1 Assessment of eosinophilia by flow cytometry.** Cytometric identification of eosinophils in
 965 the peritoneal lavage of naive and allergic mice at 3 days post-allergen challenge, based on F4/80
 966 and Siglec-F expression gated on live, singlets and CD45+ cells. Representative plots of 4
 967 independent experiments. FMO, fluorescence minus one control.

968

969

970

971

972

973

974

975

976

977

978

979

980

981

982

983

984

985

986

987

988

989

990

991

992

993

994

995

996



Fig. S2 Allergic inflammation induces a unique blood lipid profile. Heatmap of the 171 identified lipid species differentially expressed (p-value < 0.05) between allergic mice with quiescent allergy (non-challenged, blue color, n=5) and active allergy (allergen-challenged, yellow color, n=6) 7 days after challenge. The figure shows the clustering results in the form of a dendrogram. Relative lipid abundance is represented along a gradient color from blue (diminished in active allergy) to red (increased in active allergy). DG; diglycerides; Cer, ceramides; CAR, carnitines; LPE, lysophosphatidylethanolamine; LPC, lysophosphatidylcholine; PC, phosphatidylcholine; CE, cholesteryl ester; PI, phosphoinositide; LPI, lysophosphoinositide; FA, fatty acid; HerCer, hexceramide; SM, sphingomyelin; PS, glycerophosphoserines; PE, glycerophosphoethanolamines; PE-O-, oxidate glycerophosphoethanolamines; PC-O-, oxidate phosphatidylcholine; FAHFA, fatty acid esters of hydroxy fatty acids; TG, triglycerides.

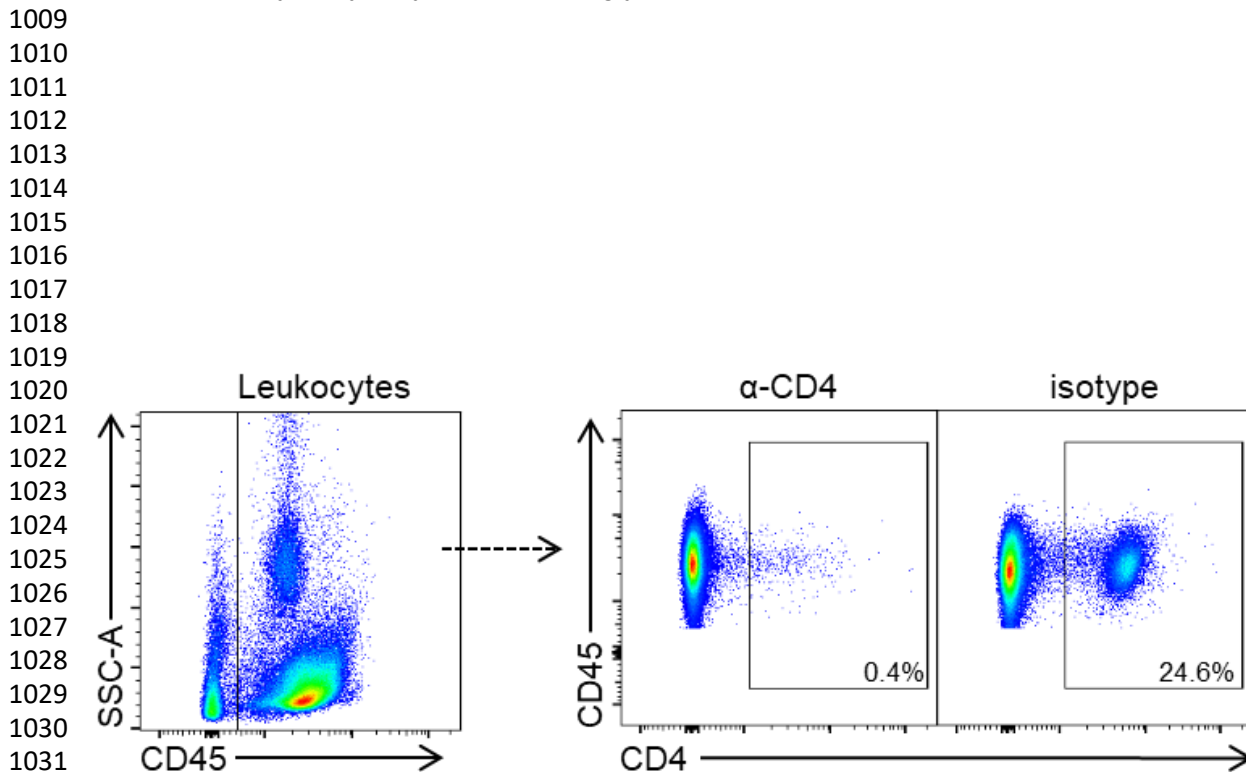


Fig. S3 Assessment of CD4 T-cell depletion by flow cytometry. Cytometric identification of CD4 T cells in the spleen of naive and allergic mice 7 days after α -CD4- (clone GK1.5) or isotype-treatment based on CD4 expression (clone RM4-5) gated on live, singlets and CD45+ cells. Representative plots of 3 independent experiments.

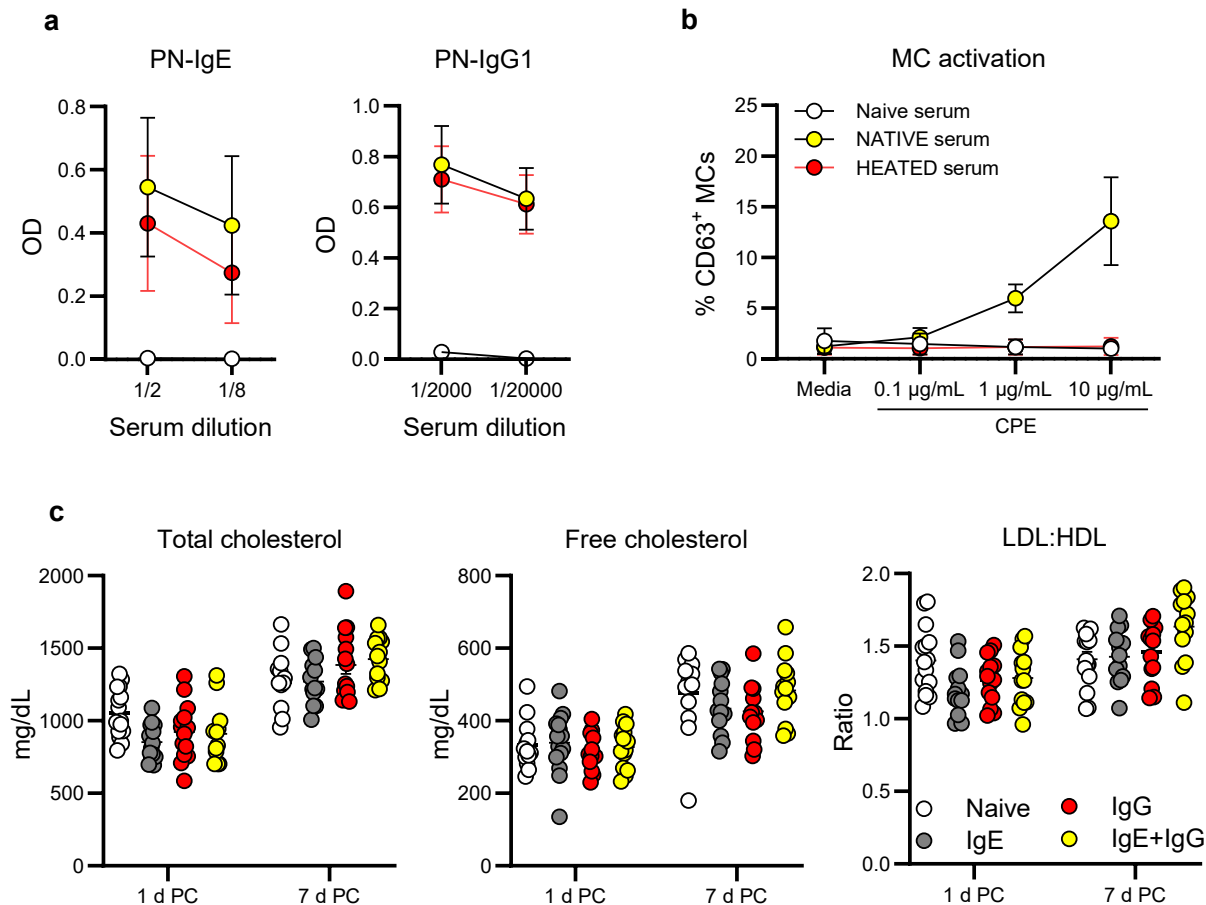


Fig. S4. Characterization of allergic sera for passive sensitization and measurement of serum lipids in circulation following allergen challenge. **a** Levels of peanut (PN)-specific IgE and IgG1 of naive and allergic sera (native or heated) used for passive sensitization. **b** Mast cell activation assays with cells sensitized with naive or allergic sera (native or heated) and challenged with different concentrations of crude peanut extract (CPE) (pooled data from 3 independent experiments). **c** Assessment of serum levels of total cholesterol, free cholesterol and LDL:HDL ratio at 1- and 7- days post-allergen challenge (PC) in passively sensitized mice with naive (n=17) or allergic sera (native or heated) to induce anaphylaxis via the classical (IgE; n=19), the alternative pathway (IgG; n=19), or both (IgE+IgG; n=18).